ACS Biomaterials SCIENCE & ENGINEERING

pubs.acs.org/journal/abseba

Review

Advanced 3D Printing Strategies for the Controlled Delivery of Growth Factors

Aurelia Poerio,* João F. Mano, and Franck Cleymand

Cite This: *ACS Biomater. Sci. Eng.* 2023, 9, 6531−6547

Read Online

ACCESS | Metrics & More | Article Recommendations

ABSTRACT: The controlled delivery of growth factors (GFs) from tissue engineered constructs represents a promising strategy to improve tissue repair and regeneration. However, despite their established key role in tissue regeneration, the use of GFs is limited by their short half-life in the *in vivo* environment, their dose-dependent effectiveness, and their space- and time-dependent activity. Promising results have been obtained both *in vitro* and *in vivo* in animal models. Nevertheless, the clinical application of tissue engineered constructs releasing GFs is still challenging due to the several limitations and risks associated with their use. 3D printing and bioprinting, by allowing the microprecise spatial deposition of multiple materials and the fabrication of complex geometries with high resolution, offer advanced strategies for an optimal release of GFs from tissue engineered constructs. This review summarizes the strategies that have been employed to include GFs and their delivery system into biomaterials used for 3D printing applications to optimize their controlled release and to improve both the *in vitro* and *in vivo* regeneration processes. The approaches adopted to overcome the above-mentioned limitations are presented, showing the potential of the technology of 3D printing to get one step closer to clinical applications.

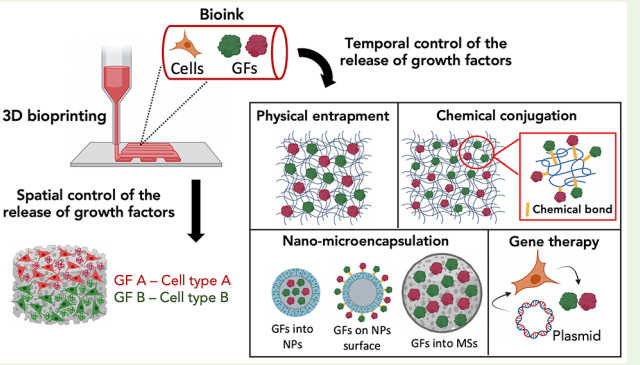

KEYWORDS: *3D bioprinting, functionalized biomaterial inks, growth factors delivery strategies*

1. INTRODUCTION

The engineering of three-dimensional biological constructs in the laboratory, with the aim of replacing damaged tissues in patients and overcoming the shortage in organ donations, is one of the primary goal of 3D bioprinting.[1] Through the precise deposition of biomaterials, living cells, and growth factors (which together form the so-called "bioink" as opposed to the "biomaterial ink" which does not include cells),[2] 3D bioprinting allows for the fabrication of structures able to closely reproduce the complex architecture of natural tissues and organs.[3] The fabrication of a new tissue *in vitro* whose functionality and properties are comparable to those of native tissue is attempted by mimicking what happens during natural regeneration and wound healing. Natural regeneration is a complex process requiring the coordinated action of different cell types and signaling molecules, such as growth factors (GFs).[4] GFs play a key role in tissue regeneration by controlling the proliferation, migration and differentiation of stem cells.[5] Therefore, the integration of GFs and their delivery system within 3D bioprinted constructs has become essential.[1] However, the optimal delivery of GFs from tissue engineered constructs presents several difficulties. A first difficulty is due to the fact that multiple GFs take part in the complex sequence of molecular and cellular events involved in the regeneration process.[6] The inclusion of multiple exogenous growth factors within a tissue engineered construct, however, would results in high cost and increased risk of adverse effects, such as ectopic tissue formation or cancer.[7,8] Second, the concentration of the delivered exogenous GFs has to be maintained in the physiological range. In fact, under-physiological dosages lead to an insufficient response, while supra-physiologic dosages cause the above-mentioned undesirable effects.[9] Finally, to exert their therapeutic role, GFs have to be released with a specific spatio-temporal pattern[10] and have to maintain their biological activity in the target location, despite their typical short-life in the *in vivo* environment.[11] Based on the above considerations, it is clear that the clinical application of GFs is particularly complex and that the therapeutic efficiency of GFs is totally dependent on the efficiency of the delivery system employed. Consequently, it

Received: June 29, 2023
Revised: October 26, 2023
Accepted: October 27, 2023
Published: November 16, 2023

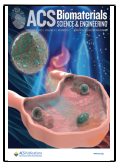

https://doi.org/10.1021/acsbiomaterials.3c00873
ACS Biomater. Sci. Eng. 2023, 9, 6531−6547

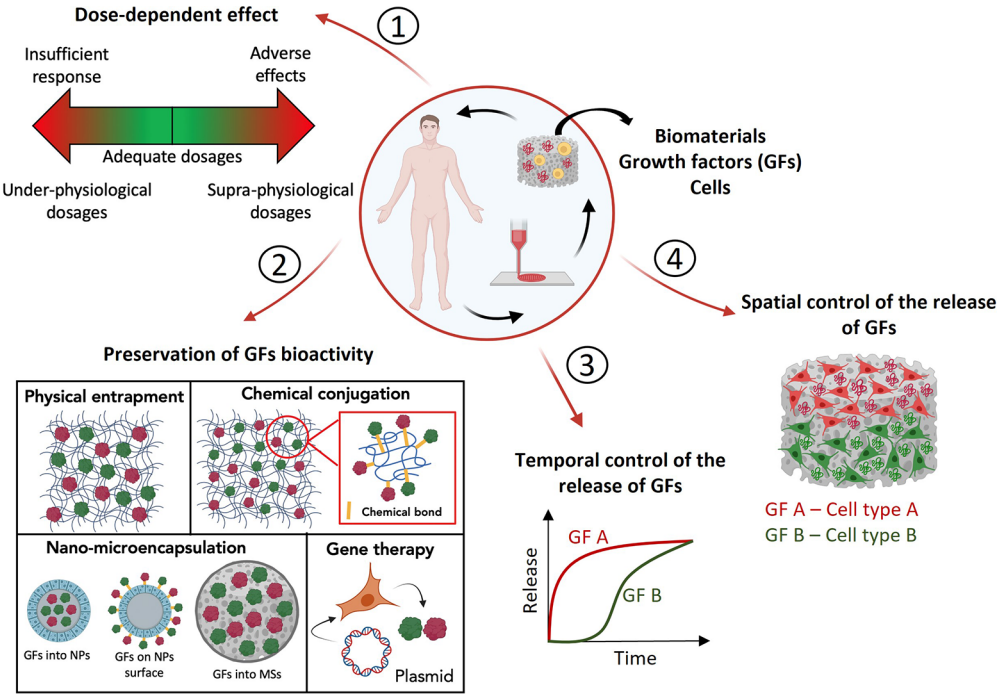

Figure 1. Schematic representation of the four levels of optimization necessary to achieve the therapeutic effect of GFs for tissue regeneration. (1) The optimal dose of GFs has to be carefully selected in order to avoid an insufficient response or side effects. (2) Based on the type of bioink and on the bioprinting process employed, a strategy should be adopted to preserve GFs bioactivity. In particular, GFs can be simply mixed within biomaterials composing inks and bioinks, be chemically conjugated to the polymer network, be encapsulated or conjugated to the surface of nanoparticles (NPs), loaded into microspheres (MSs), or their production can be induced in cells by the transfection with plasmids encoding GFs. The strategies adopted to protect GFs from the environment and preserve their bioactivity can also advantageously control their temporal release, and usually, the same strategy is chosen in order to both protect GFs bioactivity and temporally control their release. (3) The temporal control of the release of GFs and the coordination among multiple GFs is also critical since several GFs take part to the regeneration processes (*e.g.*, growth factor A: green and growth factor B: red) and their action is often time-dependent (an example is bone regeneration where angiogenesis usually precedes osteogenesis and each process is guided by different GFs). (4) The spatial distribution of GFs allows for the fabrication of complex constructs by inducing, for example, the differentiation of multiple cell types to recreate the hierarchical architecture of natural tissues. Figure created using Biorender (https://biorender.com/).

is essential to design delivery systems or to develop strategies able to provide stability, optimal activity and tunable release of GFs.[9] As well reviewed elsewhere,[9,10,12] many biomaterial-based strategies have been developed to achieve a controlled delivery of GFs. However, compared to traditional tissue engineering methods, 3D bioprinting offers extraordinary advantages such as the precise positioning of biomaterials, cells and GFs in target areas[13] and the creation of complex personalized geometries.[14] The optimal release of single or multiple GFs can be achieved by controlling different steps of the bioprinting process, starting from the choice of the biomaterials used as inks or bioinks. In fact, several parameters, such as the nature of the biomaterial, its molecular weight, its concentration and the cross-linking chemistry, can influence the bioactivity and the release of the encapsulated factors.[15] Unless incompatible with the printing process due, for example, to a drastic reduction of the printability or the clogging of the nozzle, biomaterial inks can usually be easily functionalized with GFs and their delivery systems. GFs can be simply mixed with the bioink upon formation or conjugated to the polymers constituting the bioink through chemical modifications. Alternatively, GFs can be encapsulated in advance within a delivery system, such as nano- or microparticles, which can be, in turn, incorporated into the bioink.[16] The entrapment, conjugation, and nano- or micro-encapsulation are not only primary responsible of protecting GFs from the environment but also play a major role in controlling their temporal release. The spatial location of GFs, in contrast, is usually achieved by tuning the printing parameters and by creating specific and complex designs. For example, most of the currently available 3D printers allow for the fabrication of hybrid structures by using multiple biomaterial inks. Each part of the construct could individually release a different GF in order to spatially guide the regeneration of complex tissues.[17] This review aims to discuss and summarize the strategies employed to functionalize biomaterial inks and bioinks with GFs and with their delivery system in order to control their release from 3D printed constructs and improve their efficiency. In order to obtain the desired therapeutic effect, four levels of optimization, schematized in Figure 1 and discussed in the following sections, should be taken into account. We will briefly introduce the role of GFs in tissue development and regeneration and the importance of choosing the optimal dosage of GFs when developing tissue engineered constructs in order to obtain the desired function and avoid side effects. We will then introduce two classes of biomaterials, natural and synthetic, and we will review the strategies adopted to functionalize them with GFs while preserving their bioactivity during the preparation of the ink and the printing process. Here, we will also describe a particular strategy that combines 3D printing and gene therapy giving rise to a particular class of bioinks, named GAB or "gene activated bioinks", which aim to overcome some limitations of the direct inclusion of GFs within the ink. We will then summarize the strategies employed to temporally control the release of the encapsulated GFs, such as the physical

https://doi.org/10.1021/acsbiomaterials.3c00873
ACS Biomater. Sci. Eng. 2023, 9, 6531−6547

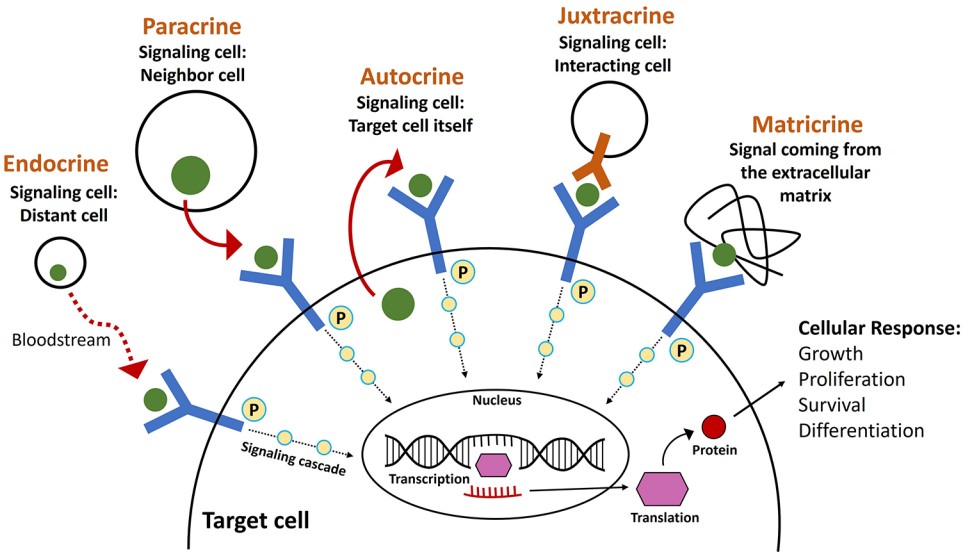

Figure 2. Mechanisms of action of growth factors. Growth factors are produced by a signaling cell and act on a target cell. Endocrine signaling is a long distance communication between a cell or group of cells (or glands) producing a soluble GF which circulates through the bloodstream to reach the target cell. Paracrine signaling occurs between neighbor cells where a soluble GF is released in the local environment. In autocrine signaling the GF is released from the target cell itself. Juxtacrine signaling occurs between cells that are physically interacting while in matricrine signaling GFs are found within the extracellular matrix. GFs in this case are not diffusing but are bound to the membrane of the signaling cell. The interaction between a GF and its receptors, located on the surface of the target cell (mostly tyrosine kinase receptors), activates a cascade of events (which usually starts with the phosphorylation of the tyrosin kinase receptor). Several factors are then activated to induce a cellular response involving the transcription and translation of proteins whose role is to influence the survival, growth, proliferation and differentiation of themselves (ex: autocrine signaling) or of other cells.

entrapment, chemical conjugation, and nano- or micro-encapsulation and how to exploit 3D printers to tune the temporal release of GFs. Finally, we will review the advantages of 3D printing technologies to control the spatial deposition of GFs presenting representative examples, with a particular emphasis on bone regeneration.

2. GROWTH FACTORS

2.1. The Problem of the Stability of Growth Factors. With the exception of estrogens, androgens, and progestogens, which are steroids, or lipid-soluble hormones, growth factors are proteins which act by binding a receptor located on the surface of cells[18] and influence cell behavior through different mechanisms of action summarized in Figure 2. Briefly, GFs are released from a signaling cell (or group of cells) and act on a target cell (a cell that express GFs receptors on its surface) through a diffusible or nondiffusible mechanism.[19,8] The target cell can be the cell that produced the growth factor (autocrine signaling) or a different one. Due to their importance in modulating the cell behavior in a very short time in order to quickly respond to external and internal stimuli, GFs naturally show a low stability, short circulating half-life and rapid rate of cellular internalization.[4] For example, the half-life of BMP-2 in blood is 1 to 4 h, while the half-life of VEGF is of only 30 min. Different strategies have been employed to improve the stability and increase the half-life of growth factors, including their chemical or genetic modification, such as site-directed mutagenesis. The latter technique has been used to either modify the GFs in the sites involved in the binding with their receptors in order to increase their half-life and availability, or to genetically remove the protease cleavage sites naturally present in growth factors and, thus, avoiding their degradation.[11] As an example of chemical modification, Lee et al.[20] improved the stability of FGF-1 through the formation of a stabilizing disulfide bond between a cysteine residue and an adjacent alanine which led to an increased mitogenic activity, increased half-life and increased thermodynamic stability. The formation of a disulfite bond allowed strengthening of the structure of the protein, improving its stability. In fact, by being mostly proteins, the functions of GFs are assured by their structure (secondary, tertiary, and quaternary),[21] which could be compromised by changes in temperature or pH, aggregation, hydrolysis of peptide bonds, oxidation of amino acid side chains, and ionic strength of the surrounding environment.[22] All these parameters have to be taken into account when preparing inks and bioinks for 3D bioprinting and when selecting the cross-linking method since they should not interfere with the activity of GFs.

2.2. The Dose-Dependent Efficiency of Growth Factors. Selecting the appropriate concentration of GFs that has to be delivered from tissue engineered constructs is of primary importance to ensure proper tissue regeneration. While the selection of the appropriate concentration of GFs is relatively easy for *in vitro* culturing systems by performing dose-finding studies, it represents a real challenge when a construct is implanted and GFs are exposed to the *in vivo* environment. There, GFs have poor stability and can easily undergo enzymatic degradation. As a consequence, supra-physiological dosages are often delivered in order to overcome these limitations. However, supra-physiological dosages can represent a risk factor leading to serious side effects such as cancer and ectopic tissue formation.[7,8,11] On the contrary, under-physiological dosages lead to an insufficient response. In order to overcome these limitations, the dosage of GFs selected through *in vitro* studies should be entirely delivered to the desired site. As we will see in the next sections, this can be done by developing strategies aiming to protect the GFs from the environment and release them in a very precise temporal and spatial manner.

https://doi.org/10.1021/acsbiomaterials.3c00873
ACS Biomater. Sci. Eng. 2023, 9, 6531−6547

3. INCLUSION OF GROWTH FACTORS INTO BIOMATERIALS USED FOR 3D PRINTING AND BIOPRINTING

Biomaterials used as inks or bioinks can be classified based on their chemical structure (such as metals, ceramics, polymers, and composites) or based on their origin which is either synthetic or natural.[23] Natural biomaterials, such as proteins, decellularized extracellular matrices, and polysaccharides, usually derive from components that are already present within the living systems (for example, some of them are components of the extracellular matrix), and therefore, they are engaged in a variety of biological processes. Consequently, they are usually not toxic, biodegradable, and able to assist cellular activities.[24] On the other hand, synthetic materials, such as organic and inorganic polymers, ceramics, and thermoplastics, have well-defined and controllable physicochemical, mechanical, and degradation properties, but they usually lack cell attachment sites. Furthermore, their processing into inks or bioinks might involve processes that are incompatible with the viability of cells and the bioactivity of growth factors, such as the use of toxic solvents and melting points higher than body temperature.[25] However, due to their remarkable properties of high printability, good control of their mechanical and degradation properties, synthetic biomaterials are highly employed for the controlled delivery of growth factors.[26] The following sections present some of the strategies used to include GFs into natural, synthetic, or hybrid biomaterials in order to protect them from the environment during the preparation of the ink and/or during the 3D printing process.

3.1. Natural Biomaterial-Based Inks and Bioinks. Inks and bioinks based on natural biomaterials (e.g., alginate, chitosan, collagen, fibrinogen, gelatin, hyaluronic acid, or laminin) offer several advantages regarding the inclusion of GFs. In fact, they are usually processed in the form of hydrogels, supporting the viability of cells and the bioactivity of the entrapped GFs. Furthermore, some of them are constituents of the extracellular matrix (ECM) and, consequently, naturally present GFs-binding domains. Accordingly, GFs can be directly mixed within the bioink upon formation, and their release depends on the diffusion and degradation profile of the hydrogel. Alternatively, GFs can be physically or chemically immobilized/conjugated to the polymer network through different strategies, such as the inclusion of heparin, which is able to bind several GFs and protect them from degradation.[27] In particular, heparin has a high negative charge density, which allows it to bind, by electrostatic forces, positive charged proteins like many GFs.[28] Furthermore, some biomaterials naturally contain GFs such as the decellularized ECM (dECM) and platelet-rich plasma (PRP). One strategy adopted to preserve the naturally present endogenous GFs, is the use of dECM as bioink.[29] Several studies showed a positive effect on tissue regeneration when using dECM with a high content of endogenous GFs[30−32] compared to other biomaterials containing exogenous GFs. This can be explained by the fact that natural ECM contains a high variety of GFs, which rarely are included in inks and bioinks from an exogenous source, due to the high cost and possible side effects. Another interesting strategy employed to include multiple GFs and avoid side effects is the inclusion of platelet-rich plasma (PRP) to hydrogel-based bioinks as a source of autologous GFs, whose positive effects have been shown by several studies.[33−38] The use of dECM as bioinks or the inclusion of PRP represent fascinating strategies to overcome the limitations of the delivery of multiple GFs in the adequate dosages from bioprinted objects, allowing for a better mimic of the *in vivo* repair and regeneration processes.[6] However, as argued above, hydrogels based on natural polymers usually present poor mechanical properties, thus reducing the shape fidelity of printed structures, and often need to be modified to allow the fabrication of complex three-dimensional bioprinted structures.

3.2. Synthetic Biomaterials. Synthetic polymers are less used as components of bioinks compared to natural ones since they usually lack biological cues for cell attachment.[39] However, they are preferred for the controlled delivery of molecules (in form of hydrogels, nano- and microspheres) and when a high resolution in 3D printing is needed.[40,41] The most used synthetic polymers are poly glycolic acid (PGA), poly lactic acid (PLA), and their copolymers PLGA, PCL, PVA, and PEG.[42] Some synthetic materials are processed in the form of hydrogels such as pluronics, poly(ethylene glycol) (PEG), or polyvinyl alcohol (PVA). However, other synthetic materials such as bioceramics (e.g., calcium phosphate cements (CPC), metals, and thermoplastics (e.g., polycarpolactone (PCL) or poly lactic-glycolic acid (PLGA)) usually require melting and curing during the fabrication steps. Since the use of high temperatures is usually incompatible with the inclusion of living cells and biological molecules,[43] different strategies have to be adopted to include GFs within high temperature bioprinted constructs in order to preserve their bioactivity. For example, Tarafder et al.[44] individually encapsulated the transforming growth factor β3 (TGF-β3), the connective tissue growth factor (CTGF), and the bone morphogenetic protein-2 (BMP-2) into PLGA microspheres (MSs) to demonstrate that the spatially controlled delivery of multiple GFs, from the same scaffold, can induce the formation of multitissue interfaces, like the temporomandibular joint (TMJ) disc, a soft cartilage disk acting as a cushioning between the bones. PLGA MSs loaded with GFs were lyophilized and subsequently filled into a high temperature cartridge containing PCL, and the constructs were printed at a temperature of 120 °C. Since the melting temperature of PLGA is around 200 °C, the encapsulated GFs were efficiently protected from denaturation and their bioactivity preserved, as confirmed by the induced *in vitro* differentiation of mesenchymal stem cells (MSCs) into fibrogenic, chondrogenic, and osteogenic cells, when exposed to CTGF, TGF-β3, and BMP-2, respectively.

3.3. Hybrid Biomaterials. In some cases, the simple mixing of GFs within bioinks is not possible or not appropriate. For example, for bone regeneration are often employed solid materials such as calcium phosphate cements (CPC), which, because of the setting reaction and subsequent leaching once the material is hydrated, can lead to the loss of the encapsulated GFs.[45,46] As a consequence, GFs can be released from CPC-based materials using different strategies, such as the inclusion of a delivery system or the combination with another material compatible with the bioactivity of GFs. To overcome this limitation, Akkineni et al.[46] encapsulated the vascular endothelial growth factor (VEGF) within dextran sulfate-chitosan microspheres which were subsequently mixed to CPC paste in a freeze-dried state. Furthemore, instead of submerging the samples in water to start the setting reaction, they placed the scaffolds in a water-saturated atmosphere (humidity), avoiding the early loss of loaded proteins. In fact, by using BSA as a model protein, they compared the amount of BSA released in PBS after 2 days from scaffolds set under both

https://doi.org/10.1021/acsbiomaterials.3c00873
ACS Biomater. Sci. Eng. 2023, 9, 6531−6547

conditions (water or humid atmosphere) and found that when set in water, 74.05 ± 5.58% of BSA was released compared to 10.32 ± 0.96% when set in a humid atmosphere. VEGF was then released slowly for 7 days, and its bioactivity was confirmed. The maintenance of the bioactivity of VEGF was confirmed through an endothelial cell proliferation assay. In another study, Ahlfeld et al.[47,48] created a biphasic scaffold through the combination of CPC paste and an alginate-gellan gum (AlgGG) bioink loaded with VEGF. CPC paste sets and hardens in contact with water forming nanocrystalline hydroxyapatite that closely resembles the natural bone mineral and shows excellent osteoconductive characteristics. As a consequence, while the CPC part provides mechanical stability to the biphasic scaffold, the AlgGG strands act as a reservoir for the release of growth factors, allowing for the vascularization of the defect region. Similarly, Shim et al.[49] used a dual-head printing system to create a biphasic scaffold made of PCL/PLGA and either collagen or gelatin, both releasing BMP-2 but, respectively, in a sustained (28 days) or faster (one week) manner. More in detail, PCL/PLGA fibers were deposited in the desired shape, forming the framework, with an empty space at the center of the scaffold which was then filled with either collagen or gelatin containing BMP-2. Their *in vivo* study showed that the slower release of BMP-2 from the collagen hydrogel strongly enhanced bone regeneration.

3.4. Gene Activated Bioinks (GABs). An interesting strategy employed to overcome the limitations of the short half-life of GFs or to sustain their release is to combine 3D bioprinting with gene therapy to induce cells to produce GFs autonomously. Viral or nonviral gene therapy allows for the delivery of plasmid DNA (pDNA) and the consequent transfection of cells in a time- and space-dependent manner within the constructs. Gene therapy combined with 3D bioprinting has been especially used for bone regeneration and the inclusion of genes, with or without their vectors, to a bioink, leads to the creation of the so called "gene activated bioinks (GABs)". Different strategies have been developed in order to increase the transfection efficiency or to induce the sustained production of GFs from cells. Some of them include the modification of the bioink itself, the inclusion of delivery systems, or the use of multiple materials. For example, Loozen et al.[50] included a naked plasmid DNA encoding for BMP-2 in a bioink composed of alginate, mesenchymal stem cells (MSCs), and calcium phosphate particles. Using a lower concentration of alginate, they obtained a higher transfection efficiency and, consequently, higher production of BMP-2 by MSCs within the bioprinted construct and enhanced osteogenetic differentiation *in vivo*. Furthermore, they showed that the fabrication of macroporous scaffolds through 3D bioprinting promotes the production of BMP-2 compared to nonporous scaffolds, proving the added value of using 3D bioprinting over other techniques. Similarly, Gonzalez-Fernandez et al.[51] found that the porosity of the scaffold modulates the transfection of cells which is faster when the porosity is higher and slower when the porosity is lower. As a consequence, in order to increase the transfection efficiency, they used a sacrificial bioink to create pores within the bioprinted constructs. By using either pro-osteogenic or prochondrogenic bioinks to create scaffolds with different porosity, they were able to direct the differentiation of encapsulated bone marrow-derived MSCs to recapitulate the native osteochondral unit. Cunniffee et al.[52] complexed plasmid DNA encoding for BMP-2 and TGF-β3 to hydroxyapatite nanoparticles, embedded in an RGD-β-irradiated alginate bioink containing bone marrow-derived MSCs. The expression of the transgenes BMP-2 and TGF-β3 was maintained for 14 days postbioprinting leading to enhanced osteogenesis of the encapsulated MSCs. In another study, Bozo et al.[53] bioprinted a construct based on octacalcium phosphate (OCP) and plasmid DNA encoding for VEGF-A. This gene-activated implant induced the differentiation of the patient's own cells in the implantation site leading to improved vascularization and osteointegration.

4. TEMPORAL CONTROL OF THE RELEASE OF GROWTH FACTORS

4.1. Physical Entrapment. The simple mixing of GFs with hydrogel-based bioinks is the most common and easiest method for their delivery from bioprinted constructs. The release kinetics of the entrapped GFs is usually characterized by an initial burst followed by a slower release which depends on the diffusion and degradation profile of the hydrogel. The diffusion process is, in turn, controlled by the properties of the matrix, i.e., the type of polymer, its molecular weight and concentration, and the characteristics of gelation.[54] Furthermore, the cross-linking density affects the degradation rate and the water content, and consequently the release of the encapsulated molecules, usually without influencing their bioactivity.[55] A fast degradation of the polymer is often related to a fast release of GFs. The strategies adopted to temporally control the release of GFs from hydrogel-based scaffold, mainly based on the optimization of the above-mentioned parameters, have been excellently reviewed.[10,12,56] Since 3D bioprinting mainly uses hydrogels as bioinks, most of the strategies employed for hydrogels are applicable to hydrogel-based 3D printed objects. However, the technology of 3D printing offers several advantages compared to traditional hydrogel-based tissue engineering strategies. In fact, it allows for a fast and reproducible deposition of single or multimaterials containing one or more GFs for the creation of complexes geometries with high resolution.[57] Furthermore, as detailed in section 4.4, it allows for a more precise selection of the macroporosity (by tuning the filament size, the defined shape, etc.) which enhances the control of the release of GFs. An example of how the choice of the material affects the release and how it can be modulated to reproduce the *in vivo* phenomena is the strategy adopted by Park et al.[58] to improve bone regeneration. The authors of the study bioprinted a multimaterial scaffold allowing for the release of VEGF and BMP-2 with two different kinetics by loading VEGF into alginate/gelatin based bioink, which degrades faster and BMP-2 in a cross-linked collagen bioink, which degrades slower. Even though information about the degradation rate of the scaffolds is not reported, the study showed that the faster release of VEGF from the implanted construct facilitated early vasculogenesis and showed promising results in enhancing the formation of bone in large size defects. However, if GFs are simply physically entrapped, they can more easily diffuse out of the construct or undergo enzymatic degradation.[16] Consequently, especially when long exposures are required, other methods can be employed to include GFs in bioinks and control their delivery, such as their immobilization or chemical conjugation to the hydrogel.

4.2. Immobilization and Covalent Conjugation. An attractive strategy employed to increase the half-life of GFs and avoid their burst release is to mimic the natural interactions between the GFs and the components of the ECM. With the aim of mimic the natural environment and particularly the ECM functions, that is where the activity of GFs is localized, different

https://doi.org/10.1021/acsbiomaterials.3c00873
ACS Biomater. Sci. Eng. 2023, 9, 6531−6547

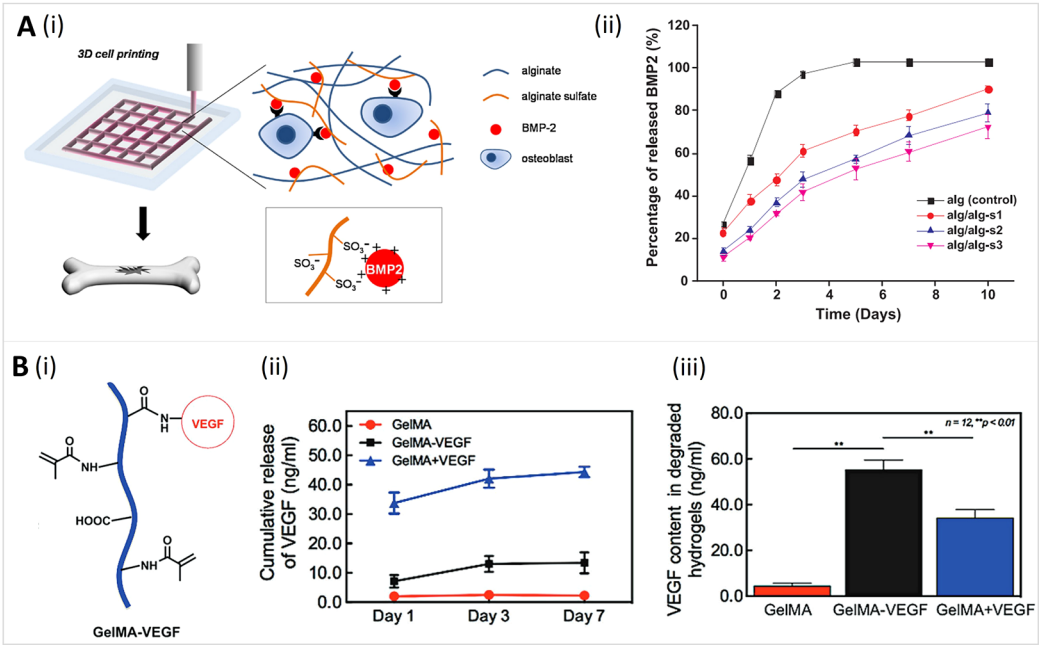

Figure 3. Covalent conjugation of GFs is used to sustain their release. (A) (i) A scheme of 3D cell printing using alginate/alginate sulfate (alg/alg-s) bioinks for the delivery of bone morphogenetic protein-2 (BMP-2). (ii) Release profiles of BMP-2 from various alginate/alginate-sulfate hydrogels during a 10-day incubation period. Reproduced from ref 61. Copyright [2018, Elsevier]. (B) (i) Structure of VEGF-conjugated GelMA hydrogels. (ii) Release of bioactive VEGF from VEGF conjugated GelMA hydrogel (GelMA-VEGF), physically mixed GelMA/VEGF hydrogel (GelMA + VEGF), and GelMA hydrogel only (GelMA). (iii) Quantification of VEGF remaining in different hydrogels after 7 days of release experiments and after degradation of the hydrogels. Reproduced from ref 63. Copyright [2017, John Wiley and Sons].

studies have reported the inclusion of heparin or heparin-sulfate within hydrogel-based bioinks[28] or the use of decellularized ECM as bioink.[29] GFs that exhibit ECM-binding domains can bind the matrix and can be presented to cells in spatio-temporal gradients that provide essential cues to elicit specific cellular responses.[27,59] In the ECM, this role is mainly due to the glycosaminoglycans such as heparin and glycoproteins such as fibronectin and laminin, and it is due to the presence of negatively charged sulfate groups which can establish electrostatic interactions with growth factors.[60] As a consequence, biomaterials can be modified to resemble the ECM. For example, the prolonged release of BMP-2 has been obtained by chemically modifying alginate, in order to produce alginate-sulfate (Figure 3A(i)). The latter, which structurally and functionally mimics the heparin, highly enhances its binding affinity to BMP-2. Furthermore, as evidenced by the release curve shown in Figure 3A(ii), the higher the concentration of alginate-sulfate, the slower the release of BMP-2. The authors suggest that this is due to the strong electrostatic interactions occurring between BMP-2 and alginate-sulfate which, in addition, protect the GF from degradation and increase its bioactivity.[61] Covalent conjugation is a common strategy used to strongly immobilize GFs to biomaterials.[62] The release of GFs mainly depends on the degradation rate of biomaterials and/or on the cleavage (hydrolytic and enzymatic) of the bonds between GFs and biomaterials. This strategy improves the stability of GFs as it may reduce the exposure of GFs to a proteolytic microenvironment at the delivery site.[11] Byamba et al.[63] chemically conjugated different concentrations of VEGF to GelMA (structure shown in Figure 3B(i)). The binding of VEGF to the polymer (GelMA-VEGF) led to a slower release of the GF, compared to the same GF simply mixed within the bioink (GelMA+VEGF (Figure 3B(ii))). This result is corroborated by the higher amount of VEGF still present in the hydrogel GelMA-VEGF after 7 days compared to the hydrogel GelMA+VEGF (Figure 3B(iii)). The slower release and consequent longer exposition to VEGF, in turn, improved the vascularization of a bone scaffold.

4.3. Encapsulation into Nano- or Microcarriers. Nano- or microencapsulation refers to the entrapment of GFs within nano- or microcarriers, usually based on biodegradable polymers.[16] The encapsulation of GFs within a nano- or microcarrier has several advantages. First of all, it protects the GFs from the environment, increasing their half-life, and allows for the encapsulation of a more precise amount of GFs, avoiding under-physiological or supra-physiological dosages which can cause undesirable effects. Furthermore, by tuning the fabrication method and the polymer properties (such as the molecular weight, the concentration, etc.), the temporal release of the entrapped factors can be significantly controlled. Nanocarriers, due to their small size, can be easily incorporated into bioinks. For microcarriers, contrariwise, the size should be carefully considered in order to avoid the clogging of the nozzle during printing.[64] The inclusion of nano- or microcarriers could also affect the viscoelastic properties of the bioinks and the resolution of the resulting biofabricated constructs in terms of printability and shape fidelity.[65] For example, laponite, a nanosilicate commonly applied for bioink reinforcement, can play the dual role of bioink reinforcer and GFs delivery system.[66] The structure of 3D bioprinted objects (e.g., filament size, geometry, macroporosity) allows for an additional control of the temporal release of GFs. Furthermore, taking advantage of the ability of 3D bioprinting to precisely localize a specific amount of bioink, the release of the GFs entrapped in nano- or microcarriers can take place under a well-controlled spatial location.

https://doi.org/10.1021/acsbiomaterials.3c00873
ACS Biomater. Sci. Eng. 2023, 9, 6531−6547

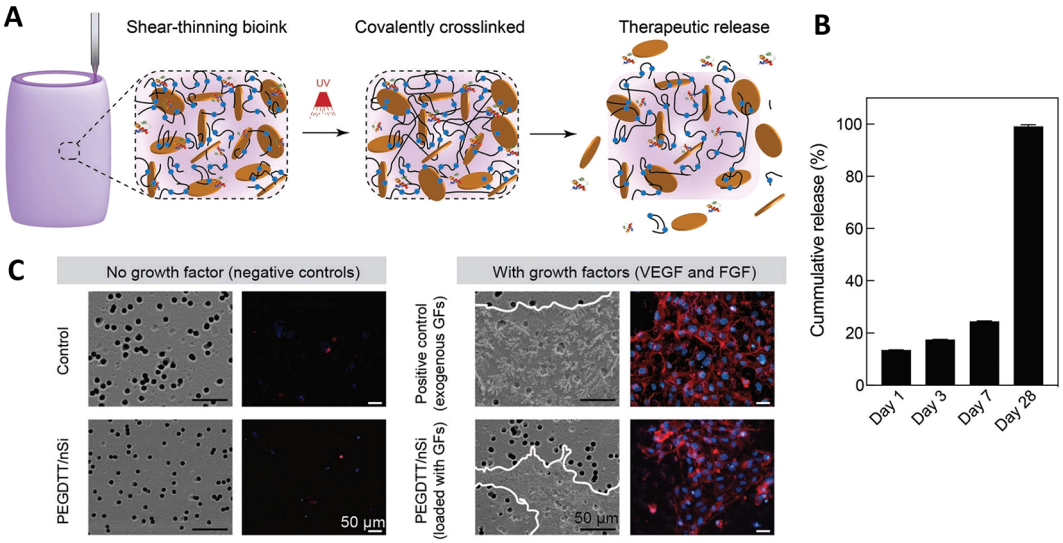

Figure 4. Nanoparticles-based temporal release of GFs from bioprinted constructs. (A) The high surface area and charged characteristics of nanosilicates allow them to sequester protein therapeutics within a 3D printing structure. The degradation of printed network results in the release of therapeutics. (B) The release of fluorescently labeled protein (FITC) from 3D printed structures was monitored over 28 days in PEGDTT/nSi hydrogels. (C) Actin and nuclei staining of migrating HUVECs across transwell. Addition of growth factors (VEGF and FGF) to PEGDTT/nSi influences the cell migration. SEM images of deposited extracellular matrix (outlined in white) are due to cell migration. Reproduced from ref 69. Copyright [2019, John Wiley and Sons].

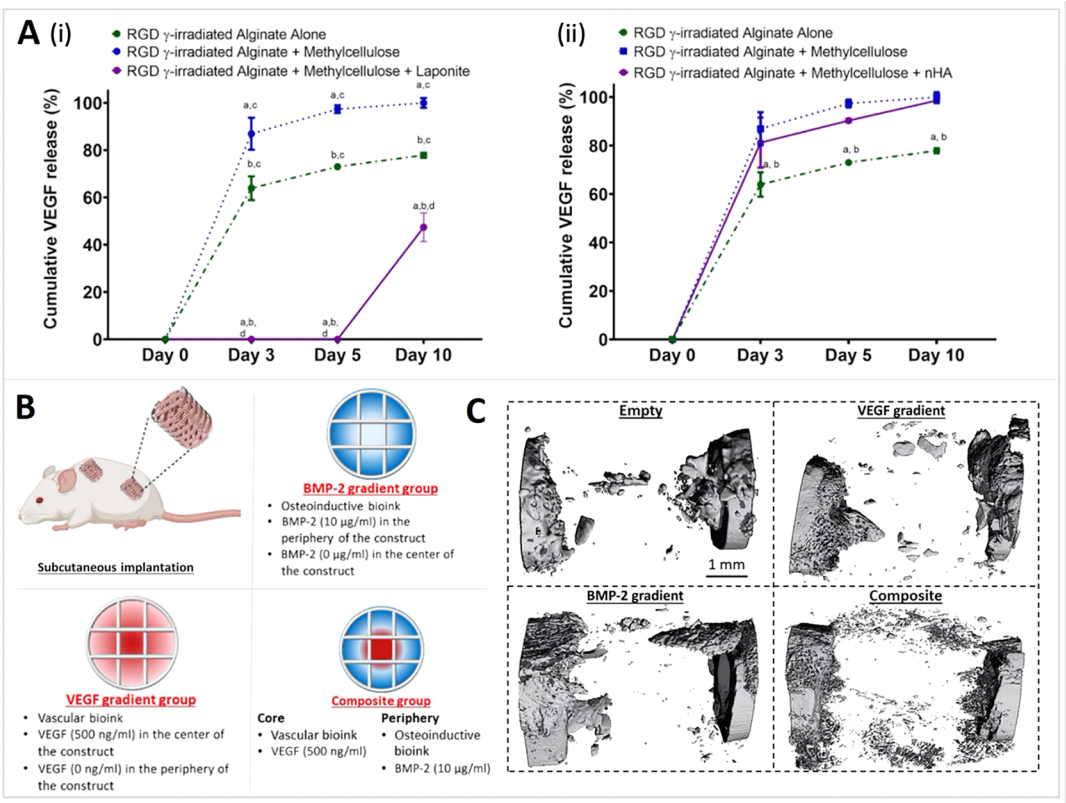

Figure 5. Spatio-temporal release of VEGF and BMP-2. (A) Cumulative release of VEGF into the media from 3D bioprinted scaffolds made of alginate and alginate + methylcellulose after the addition of laponite (i) or nanohydroxyapatite nHA (ii). (B) Schematic of the 3D printed experimental groups. (C) μ-CT reconstructed images of the defect site. Reproduced from ref 71. Copyright [2020, Science advances].

4.3.1. Nanocarriers. Due to their small size, nanoparticles (NPs) are an extremely advantageous carrier for GFs. They can provide controlled release and great ability to target the desired cells thanks to their high penetration abilities.[67] NPs are generally classified as hard and soft, with the first one having high compressive modulus and the soft ones with mechanical properties more similar to natural hydrogels.[68] In both cases, the methods usually employed to include GFs for their controlled release are their encapsulation into core−shell NPs or their conjugation/absorption to the surface of NPs.[67] For

https://doi.org/10.1021/acsbiomaterials.3c00873
ACS Biomater. Sci. Eng. 2023, 9, 6531−6547

example, nanosilicates have a particular surface charge with negatively charged faces and positively charged edges. Consequently they can interact with a wide range of GFs including BMP-2, VEGF, platelet derived growth factor (PDGF) and fibroblast derived growth factor (FGF) allowing for their sustained release. Peak et al.[69] included nanosilicates to a poly(ethylene glycol)-dithiothreitol (PEG-DTT) ink in order to both improve its shear thinning properties and act as a sustained delivery system for GFs (Figure 4A). In the first moment, they used fluorescein-conjugated bovine serum albumin (FITC-BSA) as a model protein to demonstrate that nanosilicate-loaded 3D bioprinted scaffolds could release the desired molecules for 28 days (Figure 4B). Subsequently, they demonstrated that VEGF and FGF released from 3D printed structures were able to induce the migration of human vascular endothelial cells (HUVEC) compared to the negative control groups that did not contain the GFs (Figure 4C).

Similarly, nanospheres made of polydopamine present many active functional groups on the surface that can be used to graft the GFs. Polydopamine nanospheres were used to sustain the release of CTGF and TGF-β3 up to 30 days, which led to a a significant regeneration of the intervertebral disc.[70] The use of different populations of NPs allows for the bioprinting of constructs where each part has a distinct growth factor release pattern. Freeman et al.[71] investigated the release profile of VEGF from a bioink made of RGD γ-irradiated alginate and methylcellulose in presence of laponite NPs or hydroxyapatite NPs (nHA). As shown in Figure 5A (i, ii), laponite NPs markedly slowed the release of VEGF (that was less than 50% at day 10) while nHA led to a faster and more gradual release profile (100% at day 10). Aiming to obtain a near complete release of VEGF over 10 days, in order to mimic the release observed during normal fracture healing, they included nHA to the "vascular" bioink. Contrarily, aiming to release BMP-2 from the bioprinted constructs slowly, they included laponite NPs to the "osteoinductive" bioink. The two bioinks were used to create a composite scaffold able to release BMP-2 and VEGF in a well controlled temporal and spatial manner. In particular, as shown in Figure 5B, they bioprinted four types of scaffolds, one containing no GFs, one containing a gradient of VEGF released quickly from the center of the scaffold, one releasing BMP-2 slowly from the periphery of the scaffold, and one containing both VEGF and BMP-2 in the above-mentioned spatio-temporal arrangement. Their *in vivo* results (Figure 5C) showed enhanced bone regeneration when implanting the composite scaffold. The encapsulation of GFs in the core of nanoparticles allows a controlled temporal release which is dependent on their size and on the properties of the polymers NPs are made of. Lee et al.[72] showed that the release of nerve growth factors (NGF) encapsulated into PLGA nanoparticles and subsequently embedded in PEG-based 3D bioprinted constructs, was consistently lower, for at least 7 days, compared to the release of NGF directly sprayed on the scaffolds. This sustained release of NGF from the 3D bioprinted scaffold led to enhanced neurite outgrowth compared to the NGF sprayed on the surface of the scaffold.

4.3.2. Microcarriers. The encapsulation of GFs into microcarriers is mostly referred to their inclusion in spherical structures of micrometrical size, usually labeled as microparticles (MPs) or microspheres (MSs).[12] Similar to NPs, MPs can be made of natural materials such as chitosan, alginate, and gelatin or of synthetic materials such as PLA, PLGA or PCL.[73] Either using natural or synthetic materials, the microencapsulation presents the great advantage of preserving GFs from the environment, increasing their half-life by maintaining their bioactivity, and controlling their temporal release.[74] The release profile of the encapsulated GFs is influenced by the type of material MPs are made of, its molecular weight and concentration and by its degradation profile.[75] Furthermore, it is also influenced by the material used as bioink, its degradation properties, and the geometry of the printed construct. As an example, Poldervaart et al.[76] showed that VEGF, encapsulated into gelatin MPs embedded in a bioink composed of Matrigel and alginate was released continuously for 3 weeks *in vitro* and with a slower kinetic compared to VEGF simply mixed into the bioink. The sustained release of VEGF led to a significant vasculogenic capacity *in vivo* compared to the control group (containing empty gelatin MSs) and the fast-release group (containing empty MSs and VEGF mixed in the bioink). Among the synthetic materials, MSs made of PLGA, a copolymer or PLA and PGA, are the most used and FDA-approved delivery system thanks to their versatility.[77] In fact, different properties such as the size of the MSs and their internal and external porosity can be easily modulated to obtain the desired release profile over periods ranging from a few days up to several months.[78,79] Furthermore, the different ratio of PLA to PGA (labeled as: 50/50, 75/25, 80/20, 95/5 etc.) composing the copolymer, highly influence its degradation, which is responsible of the release profile of the encapsulated molecules.[80] In particular, higher relative contents of PLA lead to a slower degradation and consequently to a slower release.[77] Based on the above, Lee et al.[81] used two different copolymers of PLGA to prepare MSs able to release CTGF and TGF-β3 for at least 42 days but with two different release profiles. More in detail, they encapsulated CTGF into PLGA MSs 50/50 and TGF-β3 into PLGA MSs 75/25 with the first one releasing the GF slower than the second one. They showed that the sequential release, *in vitro*, of CTGF for 2 weeks, followed by the release of TGF-β3 for another 2 weeks, induced the differentiation of mesenchymal stem cells into fibrochondrocyte-like cells. Subsequently, they replaced sheep meniscus with the bioprinted scaffold able to spatiotemporally release in a sequential manner CTGF and TFG-β3. Their *in vivo* study showed that the delivered GFs were able to stimulate the recruitment of stem cells into the scaffold, to induce their differentiation and *in situ* regeneration of the sheep knee meniscus. The resulting multilayer tissue composed by either fibrous and cartilaginous tissues, connected by an intermediate zone, presented comparable characteristics to the native one. Tarafder et al.,[44] contrarily, used the same type of PLGA MSs (50/50) to obtain a sustained release, *in vitro*, of multiple GFs and in particular of CTGF, TGF-β3, and BMP-2, up to 42 days. The temporally controlled delivery of CTGF and TGF-β3, *in vivo*, allowed for the formation of fibrocartilagineous tissue, similar to the native TMJ disc. Sun et al.[82] encapsulated TGF-β3 and BMP-4 into 50/50 PLGA MSs and printed a cartilage scaffold showing that the gradual release of TGF-β3 first and BMP-4 later, both sustained for at least 60 days, significantly improved *in vivo* cartilage repair.

4.4. Enhanced Temporal Control of the Release of Growth Factors through 3D Printing. The release kinetic of the entrapped molecules can be modified by tuning the printing parameters, such as the geometry of the bioprinted construct, the size of the filaments, and the distance between filaments, responsible of the macro-porosity.[28,83] Hosseinzadeh et al.[83] used this strategy to study the release of a molecule (Temozolomide - TMZ) employed for the treatment of

https://doi.org/10.1021/acsbiomaterials.3c00873
ACS Biomater. Sci. Eng. 2023, 9, 6531−6547

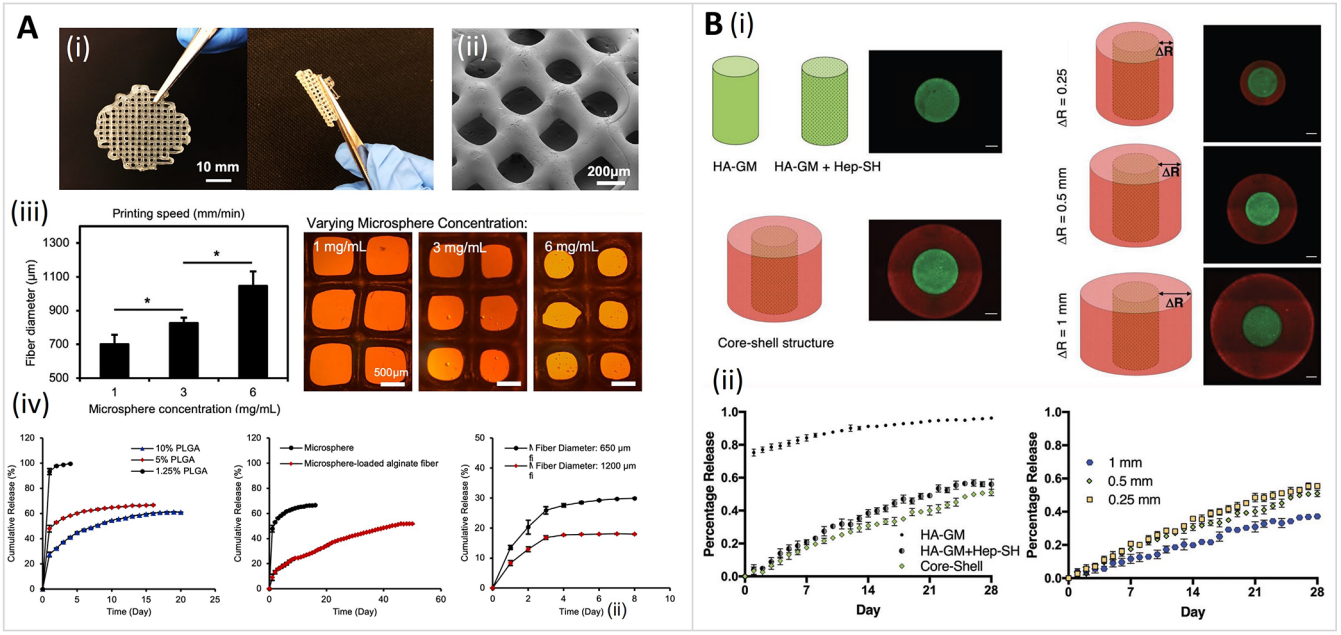

Figure 6. Tuning the printing parameters to temporally control the release of GFs. (A) Photographic (i) and SEM (ii) images of TMZ-releasing alginate mesh. (iii) Evolution of the fiber diameter with increasing concentrations of microspheres in a quantitative and qualitative way, from left to right, respectively. (iv) Release of TMZ from PLGA microspheres and 3D bioprinted scaffolds investigating the effect of PLGA concentration, the difference between microspheres only and microspheres loaded in alginate meshes, and the influence of the fiber diameter on the release of TMZ, from left to right, respectively. Reproduced from ref 83. Copyright [2019, John Wiley and Sons]. (B) (i) Design for 3D printing and structural validation with FITC (green) and TRITC-dextran (red) containing hydrogels showing cylindrical core-only structures, cylindrical core−shell structures, and core−shell structures with varied outer shell thicknesses. (ii) Release kinetics of various structures with different compositions (left) and shell thicknesses (right). Reproduced from ref 28. Copyright [2019, John Wiley and Sons].

glioblastoma. They first loaded the TMZ into PLGA microspheres and optimized the concentration of the PLGA polymer that would lead to a higher encapsulation efficiency. Subsequently they added microspheres to an alginate ink and evaluated the evolution of the diameter of alginate fibers based on the print-head pressure, the printing speed, and the concentration of microspheres (representative picture of the scaffold in Figure 6A(i, ii)). Besides showing that the filament size increases with increased print head pressure and decreased with increased speed, the authors showed that the inclusion of a higher concentration of microspheres resulted in the reduction of the viscosity of the alginate ink, leading to filaments with increased diameter (Figure 6A(iii)). Furthermore, they indicated that the printable range of microsphere concentration was from 0 to 14 mg/mL since a higher content of microspheres resulted in the clogging of the nozzle. When looking at the release profile (Figure 6A(iv)) the authors showed that lower concentrations of PLGA (1.25%) leaded to a burst release which slowed when increasing the concentration of PLGA (6 and 10%). They also showed that the release of TMZ is more sustained when microspheres are included into the hydrogel compared to MSs alone and that increasing the diameter of the alginate filaments reduces the release of the encapsulated molecule. All of these considerations have to be taken into account when including microspheres into inks and bioinks. It also must be noticed that different molecules interact with materials differently. As a consequence, the release profile can be different (and, thus adjusted) when using a different molecule and will be dependent on the type of polymer used for the fabrication of both the microspheres and/or the hydrogel and on the physicochemical properties of the encapsulated molecule or GF. Furthermore, as mentioned above, the release of the entrapped molecules can be adjusted by modeling a very precise geometry and by selecting the printing parameters and accessories such as the type of nozzle and its size. In another study, Wang et al.[28] investigated the role of the geometry of 3D printed constructs on the release of GFs by printing core + shell hydrogels made of thiolated heparin (Hep-SH) and glycidyl methacrylate hyaluronic acid (HA-GM), as shown in Figure 6B(i). More in detail, they first investigated the difference in the release of BSA between core HA-GM hydrogels and HA-GM + Hep-SH, showing that the presence of Hep-SH allowed for a significant decrease in the release compared to hydrogels only made of HA-GM. Furthermore, by printing a core (HA-GM + Hep-SH containing BSA) + shell (HA-GM + Hep-SH with no BSA) they were able to further reduce the release of BSA. Subsequently they investigated the effect of the thickness of the outer shell and in particular by creating a 1 mm, 500 μm, and 250 μm shell. As expected, the release of BSA was slower when the thickness of the shell increased (Figure 6B (ii)). In order to mimic the *in vivo* sequential release of GFs they loaded VEGF in the core and PDGF in the shell and then reversed them, showing that GFs loaded in the shell are released faster compared to GFs loaded into the core. Understanding the relationship between the scaffold geometry and GF release kinetics allows for predictive design of GF release platforms. Therefore, the author of the study developed a mathematical model capable of predicting the release of GFs (discussed below). Altogether these studies demonstrates how 3D printing can be used to fabricate user-defined structures with unique geometry in order to control the rate of GF release in hydrogels and how a precise delivery of GFs can be achieved by simply tuning the printing parameters. As another example, Lee et al.[72] printed square scaffolds with small, medium, and large square pores,

https://doi.org/10.1021/acsbiomaterials.3c00873
ACS Biomater. Sci. Eng. 2023, 9, 6531−6547

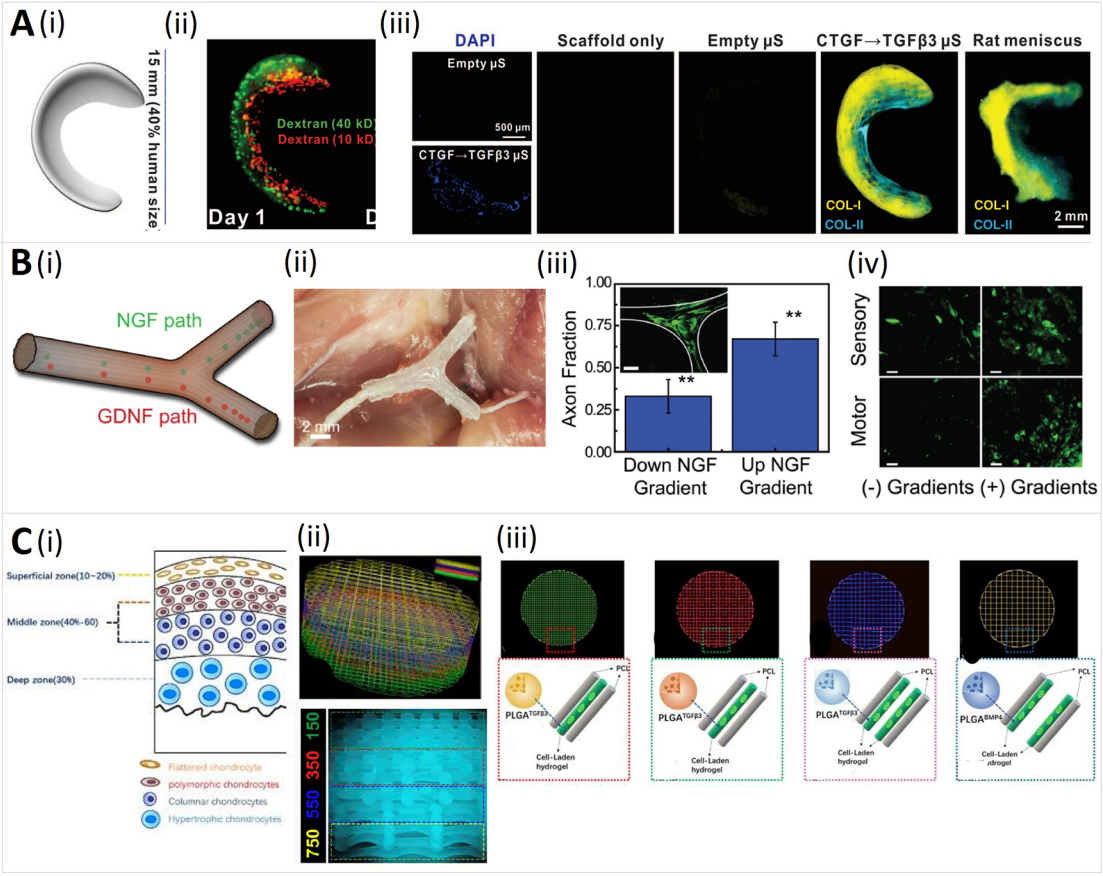

Figure 7. Spatio-temporal release of GFs from 3D-printed scaffolds. (A) (i) Anatomic reconstruction of human meniscus and 3D-printed model made of PCL. (ii) Fluorescent dextrans simulating the spatial distribution of CTGF (green, 40 kDa) and TGF-β3β3 (red, 10 kDa) within the scaffold. (iii) Expression of zone-specific collagen type I and II matrices in scaffolds incubated with human synovium MSC monolayers for 6 weeks. Reproduced from ref 81. Copyright [2014, American Association for the Advancement of Science]. (B) Functionalization of nerve pathways with path-specific biochemical gradients. In particular, the spatial distribution was obtained by printing NGF to create the sensory path and GDNF to create the motor paths in a 3D schematization (i) and after implantation (ii). (iii) Effect of the diffusive NGF gradient on the guidance of the sensory neurite network growth and (iv) histology of regenerated nerve showing cross-sections of regenerated nerves stained for tubulin (green), confirming that the presence of GFs induced the formation of different pathways. Reproduced from ref 57. Copyright [2015, John Wiley and Sons]. (C) (i) Schematization of the four-layer structure of native articular cartilage. (ii) CAD model of the gradient cartilage scaffold for the hydrogel part (top) and for the PCL pillar (lower). (iii) CAD of the four-layer with 150 μm spacing (green); 350 μm spacing (red), 550 μm spacing (blue), and 750 μm spacing(yellow), deposited between PCL paths. Reproduced from ref 82. Copyright [2020, Science advance].

corresponding to 44%, 56%, and 68% porosity, showing that scaffolds with a larger porosity significantly improve PC-12 neural cell adhesion compared to the ones with smaller porosity.

4.5. Computational Models Predicting the Release of Growth Factors. The need to precisely control the release of entrapped molecules led to the development of mathematical models able to predict the release profile of GFs from hydrogels based on (1) the composition, geometry, swelling, and degradation of the hydrogel and of the delivery system and (2) the properties of the GF itself (i.e., its molecular weight, charge, and hydrodynamic diameter). For example, Rehmann et al.[84] investigated, by using equilibrium swelling theory and rubber elasticity theory, how the concentration of the polymer (PEG) and its molecular weight influence the mesh size of the hydrogel, which is one of the main parameters affecting the release of entrapped molecules. Then, they loaded multiple proteins with a large range of size into the same hydrogel whose mesh size was previously predicted and showed that molecules with a hydrodynamic diameter bigger than the mesh size would be retained by the hydrogel, while molecules with a hydrodynamic diameter smaller than the mesh size would be released. This model allowed them to predict and then confirm experimentally that two molecules with a similar hydrodynamic diameter (in their case, BSA and PDGF) would be released with a very similar kinetic. In order to evaluate how the geometry of the hydrogels affect the release of GFs, Wang et al.[28] developed a mathematical model capable of predicting the release of BSA from core−shell structures with a unvaried core and different shell thicknesses (1 mm, 0.5 mm and 0.25 mm) which is where BSA was loaded. While they found excellent agreement for the model with a shell thickness of 1 and 0.5 mm, poor agreement was found for the model with a shell thickness of 0.25. Their hypothesis was that for a smaller shell thickness, the concentration gradient between the shell and external environment was smaller and the driving force was not enough to allow for the release of BSA, affecting the partition coefficient used in the predictive model. Despite the great advancements in computational modeling in predicting the release of molecules, it has to be considered that there will always exist a difference between the theoretical prediction and reality. In fact, the release of molecules and the behavior of hydrogels *in vivo* is strongly affected by the surrounding environment and the difficulty in

https://doi.org/10.1021/acsbiomaterials.3c00873
ACS Biomater. Sci. Eng. 2023, 9, 6531−6547

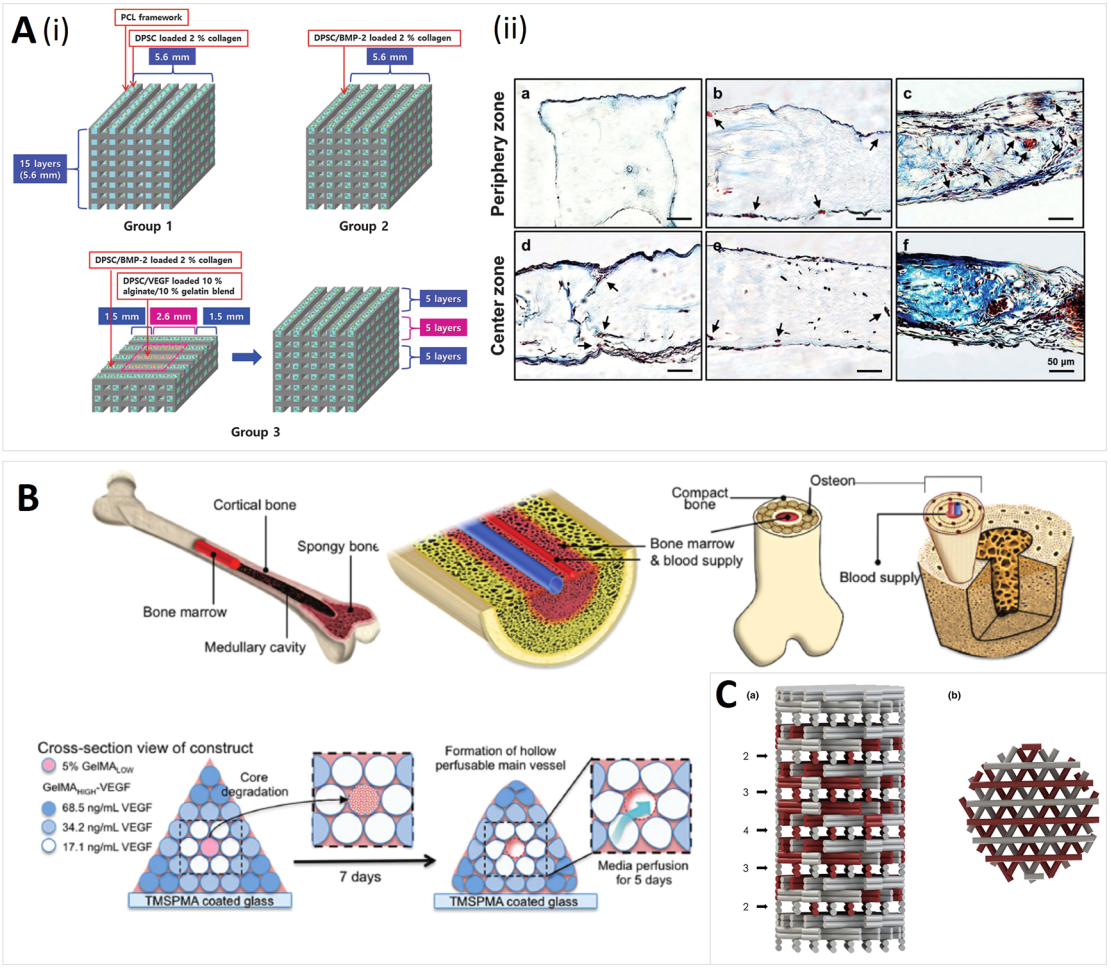

Figure 8. Control of the spatial localization of GFs within 3D bioprinted constructs for bone regeneration. (A)(i) Schematic representation of the strategy employed by Park et al.[58] to release VEGF from the inner part of the construct and BMP-2 from the periphery. (A)(ii) Masson's trichrome staining confirming bone regeneration. Blue-positive staining indicates that the encapsulated cells secreted collagenous proteins were seldom observed in group 1 (no GFs) and 2 (only BMP-2 in the periphery), while group 3 (VEGF in the center and BMP-2 in the periphery) showed strong blue staining, demonstrating the importance of prevascularization for large-volume bone regeneration. Reproduced from ref 58. Copyright [2015, The Royal Society of Chemistry]. (B) Illustrations of bone tissue structure, with a particular attention to the structure of a osteon followed by a representation of the design developed by Byambaa et al.[63] The cylindrical design aims to mimic the cylindrical structure of the osteon containing gradients of VEGF, arranged from the more concentrated on the center of the structure to the less concentrated on the periphery. Reproduced from 63. Copyright [2017, John Wiley and Sons]. (C) Model of the biphasic scaffolds with CPC (white) and the growth factor loaded hydrogel (red). The number of VEGF-loaded strands at each layer is indicated on the left side. In the center of the scaffold, four strands consist of hydrogel, which is half of the scaffold's profile. Reproduced from ref 47. Copyright [2016, Springer Nature].

integrating this aspect is the main limitation for the development of more sophisticated and precise theoretical models. However, modeling the release of growth factors from 3D bioprinted constructs and investigating computationally how the inclusion of GFs would affect the printability represent a very promising field of research that would accelerate the clinical application of 3D bioprinted constructs releasing GFs.

5. SPATIAL CONTROL OF THE RELEASE OF GROWTH FACTORS FROM 3D BIOPRINTED CONSTRUCTS

Natural tissues and organs are complex structures composed of multiple types of cells, whose activity is influenced by the macro- and microenvironments and by specific biochemical signals, such as GFs. Through the coordinated deposition of several materials, 3D bioprinting allows for the creation of structures where the distribution of cells and GFs is highly comparable to that of natural tissues.[85] A controlled spatial presentation of GFs is essential, especially for the development of heterogeneous tissues, made of multiple cell types. For example, Sun et al.[70] used three materials to create a complex intervertebral disc (IVD) scaffold. PCL was used to print the framework necessary to provide mechanical support to the IVD scaffold. The other two materials consisted of a hydrogel made of gelatin, alginate, hyaluronic acid, and glycerol containing bone marrow stromal cells (BMSCs) and polydopamine nanospheres carrying either TGF-β3 or CTGF. A specific design was then created in order to spatially control the release of TGF-β3 and CTGF, with the first one printed in the inner part of the scaffold and the second one in the periphery. The spatial distribution of these two GFs induced the corresponding BMSCs to differentiate into nucleus pulposus like cells in the inner part and annulus fibrous like cells in the periphery, suggesting the potential of the spatial organization of GFs to induce the formation of an heterogeneous tissue similar to the native one. Lee et al.[81] fabricated an acellular meniscus scaffold releasing CTGF from the inner region and TGF-β3 from the outer region. After implantation,

https://doi.org/10.1021/acsbiomaterials.3c00873
ACS Biomater. Sci. Eng. 2023, 9, 6531−6547

Table 1. Table Summarizing the Most Representative Studies Discussed in This Review[a]

tissue	GFs	delivery system	link/biolink	cross-linking of the link/biolink	cells	bioprinter	3D printing parameters	dimensions of the implanted scaffold	ref.
bone	BMP-2 VEGF	physical entrapment into the hydrogels	collagen (BMP-2) alginate/gelatin (VEGF)	2% (w/v) $CaCl_2$ for 15 min	human dental pulp stem cells (DPSCs)	custom-made (extrusion)	**PCL framework:** line width: 200 mm line height 100 mm interstrand space: 400 mm **GFs-loaded hydrogels:** dispensed between PCL lines	5.6 × 5.6 × 5.6 mm (L × W × H)	58
bone	BMP-2	electrostatic interactions between BMP-2 and alginate-sulfate	alginate/alginate-sulfate	90 mM $CaCl_2$ for 2 min	MC3T3-E1 osteoblasts *in vitro	custom-made (extrusion)	ceramic nozzle: 300 μm diameter extrusion rate: 250 mm/s	2 × 2 × 3.5 mm (L × W × H) *in vitro	61
bone	VEGF BMP-2	EDC/NHS mediated conjugation	gelatin methacryloyl	photocrosslinking	HUVECs and hMSCs	3D NovoGen MMX Organovo (extrusion)	/	each cylinder: 500 μm diameter × 10 mm long	63
bone	VEGF BMP-2	laponite (BMP-2) and hydroxyapatite HA (VEGF) NPs	RGD Y-irradiated alginate/methylcellulose	100 mM $CaCl_2$ for 1 min	acellular scaffolds for in situ tissue regeneration	RegenHU 3DDiscovery (extrusion)	**PCL framework:** nozzle: 30-gauge interstrand space: 1.2 mm **GFs-loaded hydrogels:** printed within the strands	4 mm Ø and 5 mm H	71
intervertebral disc (IVD)	CTGF TGF-β3	polydopamine nanoparticles (PDA NPs) through EDC/NHS mediated conjugation	gelatin/alginate/hyaluronic acid/glycerol	5% (w/v) $CaCl_2$ for 10 min	bone marrow-derived mesenchymal stem cells (BMSCs)	Regenove Bio-Printer-WS Hangzhou (extrusion)	**PCL framework:** metal nozzle: 330 μm, pressure: 450 kPa, temperature: 80 °C layer height 300 μm, speed 10 mm/s **GFs loaded hydrogels:** teflon nozzle: 330-μm pressure: 50 kPa temperature: 20 °C	14 mm ⌀ × 4 mm H	70
osteochondral	TGF-β3 μ_BP-2	laponite nanoclay	alginate/methylcellulose	100 mM $CaCl_2$ for 10 min	chondrocitees (cartilage zone) osteoblasts (bone zone) *in vitro	BioScaffolder 3.1 GeSiM, Germany (extrusion)	coaxial nozzle external diameter: 800 μm core diameter: 300 μm	11.5 × 11.5 mm2 with 2−4 layers *In vitro	85
osteochondral	CTGF TGF-β3	75:25 PLGA MSs	PCL	/	/	3D Bioplotter EnvisionTec, Germany (extrusion	200 μm microstrands and 200−400 μm interstrand spaces	2.5 mm ⌀ × 0.5 mm H	44
cartilage	BMP-4 TGF-β3	50:50 PLGA MSs	PCL + hydrogel (gelatin, fibrinogen, hialuronic acid)	/	mesenchymal stem cell (MSC)	OPUS (Novaprint) (extrusion)	**PCL framework:** nozzle size: 200 μm, layer thicknes: 200 μm, speed: 180 mm/min,fiber spacing: increasing gradually from 150 to 750 **GFs-loaded hydrogels:** printed within the strands Nozzle: 100 μm	4 × 4 × 4 mm for (rabbit-scale) *implanted 14 × 14 × 14 mm (human-scale)	82
knee meniscus	CTGF TGF-β3	50:50 PLGA MSs (CTGF) 75:25 PLGA MSs (TGF-β3)	PCL	/	in situ	3DBioplotter EnvisionTEC, Germany (extrusion)	300-mm microstrands 100-mm microchannels	anatomic meniscus	81
nerve	NGF	PLGA NPs	PEG/PEG-DA	photopolymerization (UV)	PC-12 and primary rat cortical neurons in vitro	SL-based 3D printing Printrbot* (stereolitography	printing speed: 25 mm/s laser spot diameter: 190 ± 50 μm	8 mm diameter in vitro	72
nerve	NGF GDNF	hydrogel	gelatin methacrylate	photopolymerization (UV)	acellular scaffolds for in vivo sudy	custom-made (extrusion)	printing speed range: 0.1−1 mm s−1	10 mm length	57
vascular	VEGF	gelatin micropartices	matrigel/alginate	100 mM $CaCl_2$ for 15 min	human endothelial progenitor cells (EPCs)	Bioscaffolder (GeSiM, Germany	/	10 × 10 × 3 mm (L × W × H)	76

[a]If not mentioned otherwise, all the information reported in the table concerns scaffolds used for *in vivo* studies.

https://doi.org/10.1021/acsbiomaterials.3c00873
ACS Biomater. Sci. Eng. 2023, 9, 6531−6547

they found that the outer zone of the regenerated meniscus was populated by fibroblast-like cells, the inner one by chondrocyte-like cells while mixed fibroblast- and chondrocyte-like cells were found in the intermediate zone, as previously also confirmed *in vitro* by comparing the scaffold exposed to human synovium MSC monolayers for 6 week to the native rat meniscus (Figure 7A(i - iii)). This study demonstrates not only the power of GFs in influencing the behavior of cells but also their ability to attract endogenous stem cells and induce their differentiation *in situ*. 3D bioprinting is also showing progresses in the field of neural tissue regeneration by improving the traditional nerve guidance conduits through the microprecise deposition of single or multiple GFs gradients.[86] For example, Johnson et al.[57] fabricated a bifurcate pathway (Figure 7B(i–iv)) with one path loaded with a gradient of NGF to induce the growth of sensory nerves and the other path loaded with a gradient of GDNF to induce the growth of motor nerves. Both GFs were physically entrapped into a gelatin methacrylate hydrogel and released via a diffusive mechanism for 3 weeks. This bifurcated platform aims not only to achieve the regeneration of damaged nerve plexuses but also to enhance the fundamental understanding of neuronal regeneration. Sun et al.[82] developed a dual-factor releasing system with a well defined spatial organization for cartilage regeneration. As shown in Figure 7C(i), the native joint cartilage is characterized by multiple layers with a precise zonal-dependent chondrogenic differentiation and ECM deposition (which is higher in the superficial zone and lower in the deep zone). In order to obtain this gradient, they encapsulated TGF-β3 and BMP-4 into PLGA MSs, to sustain their release for 60 days (*in vitro*) and created a four-layers construct (Figure 7C(ii)). Three of the layers contained MSCs and TGF-β3-loaded PLGA MSs while the fourth layer contained MSCs and BMP-4-loaded MSs. Furthermore, in order to improve the integration of the cartilaginous constructs, the four layers were fabricated with increasing spacing between the printed filaments for each layer (Figure 7C(iii)), ranging gradually from 150 μm (in the superficial zone) to 750 μm (in the deepest zone) to maximize the diffusion of nutrients. The spatiotemporal controlled delivery of TGF-β3 and BMP-4, combined to a strategical design with a controlled microporosity, allowed for the fabrication of a highly complex anisotropic cartilage construct which showed, *in vivo*, high similarity to the native tissue.

Due to the incidence of bone disorders worldwide, many studies are focusing on the regeneration of large bone defects through the controlled delivery of GFs using 3D bioprinting strategies.[87] Bone is a complex, highly vascularized tissue. Vascularization is of great importance since, during bone regeneration, osteogenesis is preceded by angiogenesis.[88,89] For the regeneration of large size defects of bone, it is then essential that both processes occur.[90,91] For this reason, several studies focused on the delivery of VEGF, which is the most potent inducer of angiogenesis and BMP-2, known to strongly promote osteogenesis.[92,93] The positive effect of their delivery, either in combination or alone, has been largely demonstrated through traditional tissue engineering approaches.[94−96] However, significant improvements in bone regeneration were obtained using 3D bioprinting technologies since they allow for the use of multiple materials and the fabrication of high resolution geometries. For example, Park et al.[58] obtained a spatiotemporal control on the delivery of VEGF and BMP-2 by using two different biomaterials as bioink, one releasing VEGF faster and another one releasing BMP-2 slower and by 3D printing the two materials in a precise spatial organization. In particular, they printed human dental pulp stem cells (DPSCs), that have both osteogenic and vasculogenic potential, with VEGF in the center of the 3D constructs to induce a prevascularization of the tissue and BMP-2 in the peripheral zone (Figure 8A(i)). Their *in vivo* study, consisting of three groups (group 1 containing no GFs, group 2 releasing only BMP-2 from the periphery and group 3 releasing VEGF form the center and BMP-2 from the periphery) showed that the prevascularized implanted scaffolds, due to the presence of VEGF and DPSCs, led to an improved bone regeneration compared to the same scaffold non prevascularized (Figure 8A(ii)). Contrariwise, Freeman et al.[71] functionalized a same bioink with two different GFs-loaded nanoparticles as delivery system (hydroxyapatite for VEGF and laponite for BMP-2). Similarly, they placed the bioink containing VEGF in the inner part of the structure and BMP-2 in the periphery. They showed that the spatial patterning of VEGF and BMP-2 enhanced angiogenesis *in vivo* leading to improved large bone defect healing. Byambaa et al.[63] printed cylinders with different concentrations of VEGF (covalently conjugated to GelMA) gradients, arranging them from a higher concentration on the center of the structure to a lower concentration on the periphery. More in detail, and as shown in Figure 8 B, the central rod of the construct was printed using VEGF conjugated GelMA with low methacryloyl substitution (GelMA-LOW) containing HUVECs and hMSCs. Then, three layers of cylinders were printed around this soft core using GelMA with a high degree of substitution (GelMA-HIGH) loaded with silicate nanoplatelets to induce osteogenic differentiation of hMSCs into osteoblasts and containing three different concentrations of covalently conjugated VEGF (68.5, 34.2, 17.1 ng/mL). The softness of the inner core led to a fast degradation of the hydrogel, leaving an open lumen and a perfusable channel of 500 μm after 12 days of *in vitro* incubation functioning as the central blood vessel of the cell-laden construct. Ahlfeld et al.[47,48] created a biphasic scaffold based on a combination of CPC paste and VEGF-loaded alginate-based hydrogel and established a gradient of VEGF by increasing the number of VEGF-loaded hydrogel strands per layer in the center of the construct and by lowering it in the periphery of a cylindrical scaffold (Figure 8C). The spatial organization of VEGF showed a significant enhancement of the vascularization of the implanted scaffold compared to the groups that did not contain VEGF.

5.1. 3D Bioprinting Tools as Innovative GFs Delivery Strategies. Most common 3D bioprinting techniques comprise extrusion-based bioprinting, inkjet bioprinting, stereolithography-based bioprinting, and laser-assisted bioprinting. The differences among these technologies depend on the target design, on the type of biomaterials that can be used as inks or bioinks and on the need of a specific cell density.[3] To date, due to its high versatility and large choice of biomaterials that can be used as bioink, extrusion-based 3D bioprinting is the most used technique. Table 1 summarizes the application, the type of GFs and delivery system used in the most representative studies discussed in this review, as well as the type of ink/bioink, the type of bioprinter, and the geometry of the scaffolds. Besides tuning the bioprinting parameters as discussed above, singular approaches for the spatial delivery of GFs have been explored based on the use of tools for 3D bioprinting such as the coaxial nozzle.[97] This tool was developed in the first place for electrospinning in order to keep fresh solvent around the nozzle to prevent clogging. For extrusion based bioprinting, coaxial nozzles have been widely used to extrude the bioink from the

https://doi.org/10.1021/acsbiomaterials.3c00873
ACS Biomater. Sci. Eng. 2023, 9, 6531−6547

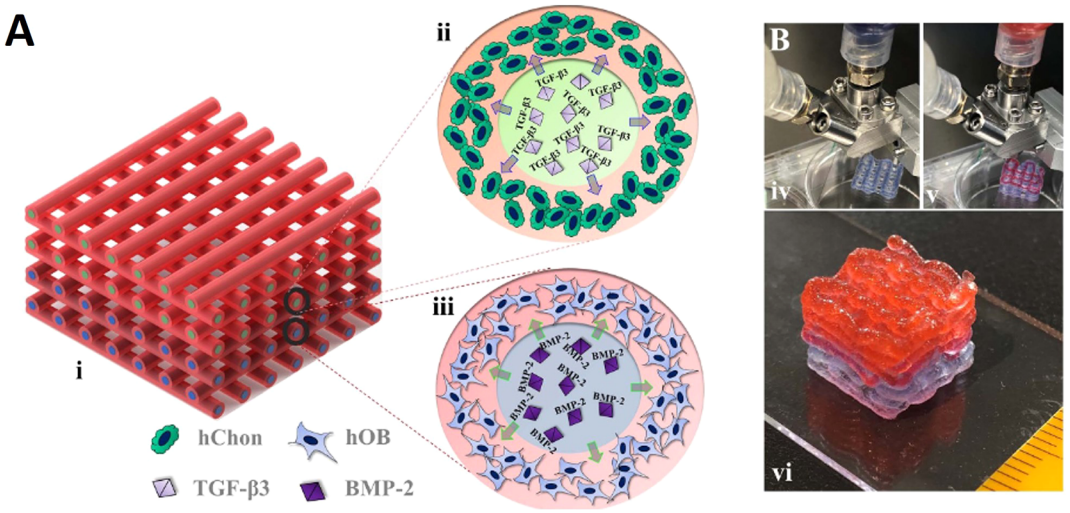

Figure 9. Schematic of the core−shell system with two coaxially extruded zones (i): upper zone containing human articular chondrocytes (hChon) in the shell and TGF-β 3 in the core compartment and a bone zone loaded with human preosteoblasts (hOB) in the shell and BMP-2 in the core. (B) Pictures of the multizonal core−shell printing made visible with a blue-dyed core for the bone zone and a red-dyed core for the cartilage zone. Reproduced from ref 85. Copyright [2022, IOP Publishing].

core and its cross-linker solution from the shell so that the immediate cross-linking assures to the 3D printed construct the required mechanical strength. For example, Zhang et al.[98] used a coaxial nozzle in order to create vasculature conduits. More in detail, they loaded human umbilical vein smooth muscle cells (HUVSMCs) into an alginate hydrogel and dispensed it through the shell of the coaxial nozzle while a solution of $CaCl_2$ was dispensed through the core section. By doing that, when alginate and $CaCl_2$ were in contact, cross-linking started immediately forming conduits. Kilian et al.[85] used a coaxial nozzle to create concentric compartments within one single strand, allowing for a very precise local delivery of cells and GFs, for the formation of the osteochondral region. More in particular, and as shown in Figure 9, they created bizonal constructs composed of a cartilage zone containing human articular chondrocytes (hChon) in the shell and TGF-β 3 in the core compartment and a bone zone loaded with human preosteoblasts (hOB) in the shell and BMP-2 in the core. Both parts, the shell and the core, were made of an alginate-methylcellulose bioink containing laponite in the core part to allow for the sustained release of GFs. Though a series of highly specific *in vitro* studies, they showed that the local supply of GFs was sufficient to induce the differentiation of cells without disturbing the differentiation of cells located in the other zone of the scaffold. This strategy eliminates the need of applying GFs within the culture medium. Furthermore, it allows for the loading of a much more controlled amount of GFs, avoiding under or supra physiological dosages and allowing for a very precise spatial delivery of GFs. Furthermore, this strategy also allows to combine biomaterials with different mechanical properties in which the stiffer one supports the softer one.[99]

6. CONCLUSIONS AND FUTURE OUTLOOK

The therapeutic efficiency of growth factors in tissue repair and regeneration has been largely demonstrated. However, there are still several limitations for the clinical applications of biomaterials releasing GFs due to their complex mechanism of action and high risk of side effects. The number of growth factors intervening, *in vivo*, in tissue repair and regeneration is very high, and their action is strictly regulated by the activity of cells and extracellular matrix components, which determine their precise spatio-temporal release. Currently, a growing number of studies are focused on the improvement of bioink properties and on the development of new delivery systems to be able to reproduce, *in vitro*, the complex natural mechanism of action of GFs. Many strategies for a more controlled delivery of GFs can be developed using the existing 3D bioprinting methods and tools or through the development of new concepts. The deposition of multiple and specialized biomaterials, able to release single or multiple GFs in a temporal and spatial controlled manner could allow for the use of appropriate dosages of GFs, increasing the efficacy and safety of bioprinted constructs. This, along with the possibility to recreate precise anatomical and individualized shapes through medical imaging techniques, makes 3D printing or bioprinting a very promising tool for clinical tissue engineering applications. To date, the clinical application of tissue engineered products containing growth factors is limited and more or less complex. In fact, since tissue engineered products can be made of a combination of biomaterials, cells and growth factor, each of this component is subject to its own regulation and must prove its safety. Based on to their origin (autologous, allogenic, xenogenic, etc.) and degree of manipulation to generate tissue engineered products, cells represent the factor whose regulation is the most stringent and that raise more ethical concerns.[100] It appears then logic that the more complex a tissue engineered system is, the more time and regulatory steps are required to translate research into clinical application. In order to maximize the safety of the released growth factors, more work will be needed from the biomaterials side to better control their release, including the use of multiscale delivery systems (e.g., nanoparticles in microparticles or stratified structures) and improved methodologies for stabilizing the structure of GFs compliant with the bioprinting process. Furthermore, the use of modeling tools to predict the release of the factors from complex structures will most probably gain relevance in the future; by reversing engineering, this could be useful in the design of customizable bioprinted devices with the required release of the cargo in time and space. However, at the time, many studies do not detail some useful information, such as the duration of the printing process, which together with the fact that usually small animal models are used for these studies makes it difficult to evaluate

https://doi.org/10.1021/acsbiomaterials.3c00873
ACS Biomater. Sci. Eng. 2023, 9, 6531−6547

the feasibility of fabricating large-organ scale models. Another limitation of some studies is the lack of information concerning the degradation of scaffolds in a dynamic environment. Such a dynamic environment could be simulated by using bioreactors or microfluidic devices that, by mimicking body fluids, could also allow to study the release of GFs in a more *in vivo*-like environment.

AUTHOR INFORMATION

Corresponding Author

Aurelia Poerio − *Institut Jean Lamour, University of Lorraine, Nancy 54011, France;* orcid.org/0000-0002-4201-377X; Email: aurelia.poerio@univ-lorraine.fr

Authors

João F. Mano − *Department of Chemistry, CICECO—Aveiro Institute of Materials, University of Aveiro, Aveiro 3810-193, Portugal;* orcid.org/0000-0002-2342-3765

Franck Cleymand − *Institut Jean Lamour, University of Lorraine, Nancy 54011, France*

Complete contact information is available at: https://pubs.acs.org/10.1021/acsbiomaterials.3c00873

Notes

The authors declare no competing financial interest.

ACKNOWLEDGMENTS

This work was developed within the scope of the project CICECO-Aveiro Institute of Materials, UIDB/50011/2020 and UIDP/50011/2020, financed by national funds through the Portuguese Foundation for Science and Technology/MCTES. This work was also supported by the French PIA project "Lorraine Université d'excellence", reference ANR-15-IDEX-04-LUE and by CNRS GDR 2088 "BIOMIM".

REFERENCES

(1) Skardal, A. Bioprinting essentials of cell and protein viability. In *Essentials of 3D Biofabrication and Translation*; Elsevier, 2015; pp. 1−17.

(2) Groll, J.; Burdick, J. A.; Cho, D.-W.; Derby, B.; Gelinsky, M.; Heilshorn, S. C.; Juengst, T.; Malda, J.; Mironov, V. A.; Nakayama, K.; et al. A definition of bioinks and their distinction from biomaterial inks. *Biofabrication* **2019**, *11* (1), 013001.

(3) Murphy, S. V.; Atala, A. 3d bioprinting of tissues and organs. *Nature biotechnology* **2014**, *32* (8), 773−785.

(4) Mitchell, A. C.; Briquez, P. S.; Hubbell, J. A.; Cochran, J. R. Engineering growth factors for regenerative medicine applications. *Acta biomaterialia* **2016**, *30*, 1−12.

(5) Barrientos, S.; Stojadinovic, O.; Golinko, M. S.; Brem, H.; Tomic-Canic, M. Growth factors and cytokines in wound healing. *Wound repair and regeneration* **2008**, *16* (5), 585−601.

(6) Chen, F.-M.; Zhang, M.; Wu, Z.-F. Toward delivery of multiple growth factors in tissue engineering. *Biomaterials* **2010**, *31* (24), 6279−6308.

(7) James, A. W.; LaChaud, G.; Shen, J.; Asatrian, G.; Nguyen, V.; Zhang, X.; Ting, K.; Soo, C. A review of the clinical side effects of bone morphogenetic protein-2. *Tissue Engineering Part B: Reviews* **2016**, *22* (4), 284−297.

(8) Witsch, E.; Sela, M.; Yarden, Y. Roles for growth factors in cancer progression. *Physiology* **2010**, *25*, 85.

(9) Subbiah, R.; Guldberg, R. E. Materials science and design principles of growth factor delivery systems in tissue engineering and regenerative medicine. *Advanced healthcare materials* **2019**, *8* (1), 1801000.

(10) Whitaker, M.; Quirk, R.; Howdle, S.; Shakesheff, K. Growth factor release from tissue engineering scaffolds. *Journal of Pharmacy and Pharmacology* **2010**, *53* (11), 1427−1437.

(11) Ren, X.; Zhao, M.; Lash, B.; Martino, M. M.; Julier, Z. Growth factor engineering strategies for regenerative medicine applications. *Frontiers in bioengineering and biotechnology* **2020**, *7*, 469.

(12) Caballero Aguilar, L. M.; Silva, S. M.; Moulton, S. E. Growth factor delivery: defining the next generation platforms for tissue engineering. *J. Controlled Release* **2019**, *306*, 40−58.

(13) Cui, H.; Nowicki, M.; Fisher, J. P.; Zhang, L. G. 3d bioprinting for organ regeneration. *Advanced healthcare materials* **2017**, *6* (1), 1601118.

(14) Beski, D.; Dufour, T.; Gelaude, F.; Ilankovan, A.; Kvasnytsia, M.; Lawrenchuk, M.; Lukyanenko, I.; Mir, M.; Neumann, L.; Nguyen, A. et al. Software for biofabrication. In *Essentials of 3D Biofabrication and Translation*; Elsevier, 2015; pp. 19−41.

(15) Gungor-Ozkerim, P. S.; Inci, I.; Zhang, Y. S.; Khademhosseini, A.; Dokmeci, M. R. Bioinks for 3d bioprinting: an overview. *Biomaterials science* **2018**, *6* (5), 915−946.

(16) Wang, Z.; Wang, Z.; Lu, W. W.; Zhen, W.; Yang, D.; Peng, S. Novel biomaterial strategies for controlled growth factor delivery for biomedical applications. *NPG Asia Materials* **2017**, *9* (10), No. e435.

(17) Ashammakhi, N.; Ahadian, S.; Xu, C.; Montazerian, H.; Ko, H.; Nasiri, R.; Barros, N.; Khademhosseini, A. Bioinks and bioprinting technologies to make heterogeneous and biomimetic tissue constructs. *Materials Today Bio* **2019**, *1*, 100008.

(18) Stone, W. L.; Leavitt, L.; Varacallo, M. Physiology, growth factor. *StatPearls*; StatPearls Publishing: Treasure Island, FL, 2017.

(19) Tada, S.; Kitajima, T.; Ito, Y. Design and synthesis of binding growth factors. *International Journal of Molecular Sciences* **2012**, *13* (5), 6053−6072.

(20) Lee, J.; Blaber, M. Increased functional half-life of fibroblast growth factor-1 by recovering a vestigial disulfide bond. *Journal of Proteins & Proteomics* **2010**, *1* (2), 37−42.

(21) Bradshaw, R. A.; Murray-Rust, J.; Blundell, T. L.; Mcdonald, N. Q.; Lapatto, R.; Ibáñez, C. F. Nerve growth factor: structure/function relationships. *Protein Sci.* **1994**, *3* (11), 1901−1913.

(22) Arakawa, T.; Prestrelski, S. J.; Kenney, W. C.; Carpenter, J. F. Factors affecting short-term and long-term stabilities of proteins. *Advanced drug delivery reviews* **2001**, *46* (1−3), 307−326.

(23) Marin, E.; Boschetto, F.; Pezzotti, G. Biomaterials and biocompatibility: An historical overview. *Journal of Biomedical Materials Research Part A* **2020**, *108* (8), 1617−1633.

(24) Mano, J.; Silva, G.; Azevedo, H. S.; Malafaya, P.; Sousa, R.; Silva, S. S.; Boesel, L.; Oliveira, J. M.; Santos, T.; Marques, A.; et al. Natural origin biodegradable systems in tissue engineering and regenerative medicine: present status and some moving trends. *Journal of the Royal Society Interface* **2007**, *4* (17), 999−1030.

(25) Khoeini, R.; Nosrati, H.; Akbarzadeh, A.; Eftekhari, A.; Kavetskyy, T.; Khalilov, R.; Ahmadian, E.; Nasibova, A.; Datta, P.; Roshangar, L.; et al. Natural and synthetic bioinks for 3d bioprinting. *Advanced NanoBiomed Research* **2021**, *1* (8), 2000097.

(26) Koons, G. L.; Mikos, A. G. Progress in three-dimensional printing with growth factors. *J. Controlled Release* **2019**, *295*, 50−59.

(27) Sakiyama-Elbert, S. E. Incorporation of heparin into biomaterials. *Acta biomaterialia* **2014**, *10* (4), 1581−1587.

(28) Wang, P.; Berry, D.; Moran, A.; He, F.; Tam, T.; Chen, L.; Chen, S. Controlled growth factor release in 3d-printed hydrogels. *Advanced healthcare materials* **2020**, *9* (15), 1900977.

(29) Dzobo, K.; Motaung, K. S. C. M.; Adesida, A. Recent trends in decellularized extracellular matrix bioinks for 3d printing: an updated review. *International journal of molecular sciences* **2019**, *20* (18), 4628.

(30) Kim, B. S.; Kwon, Y. W.; Kong, J.-S.; Park, G. T.; Gao, G.; Han, W.; Kim, M.-B.; Lee, H.; Kim, J. H.; Cho, D.-W. 3d cell printing of in vitro stabilized skin model and in vivo pre-vascularized skin patch using tissue-specific extracellular matrix bioink: a step towards advanced skin tissue engineering. *Biomaterials* **2018**, *168*, 38−53.

(31) Ali, M.; Pr, A. K.; Yoo, J. J.; Zahran, F.; Atala, A.; Lee, S. J. A photo-crosslinkable kidney ecm-derived bioink accelerates renal tissue formation. *Advanced healthcare materials* **2019**, *8* (7), 1800992.
(32) Won, J.-Y.; Lee, M.-H.; Kim, M.-J.; Min, K.-H.; Ahn, G.; Han, J.-S.; Jin, S.; Yun, W.-S.; Shim, J.-H. A potential dermal substitute using decellularized dermis extracellular matrix derived bio-ink. *Artificial cells, nanomedicine, and biotechnology* **2019**, *47* (1), 644−649.
(33) Santos, S. C.; Custódio, C. A.; Mano, J. F. Photopolymerizable platelet lysate hydrogels for customizable 3d cell culture platforms. *Advanced healthcare materials* **2018**, *7* (23), 1800849.
(34) Ahlfeld, T.; Cubo-Mateo, N.; Cometta, S.; Guduric, V.; Vater, C.; Bernhardt, A.; Akkineni, A. R.; Lode, A.; Gelinsky, M. A novel plasma-based bioink stimulates cell proliferation and differentiation in bioprinted, mineralized constructs. *ACS applied materials & interfaces* **2020**, *12* (11), 12557−12572.
(35) Lubkowska, A.; Dolegowska, B.; Banfi, G. Growth factor content in prp and their applicability in medicine. *J Biol Regul Homeost Agents* **2012**, *26* (2 Suppl 1), 3S−22S.
(36) Tavares, M.; Santos, S.; Custódio, C.; Farinha, J.; Baleizão, C.; Mano, J. Platelet lysates-based hydrogels incorporating bioactive mesoporous silica nanoparticles for stem cell osteogenic differentiation. *Materials Today Bio* **2021**, *9*, 100096.
(37) Irmak, G.; Gümüşderelioğlu, M. Photo-activated platelet-rich plasma (prp)-based patient-specific bio-ink for cartilage tissue engineering. *Biomedical Materials* **2020**, *15* (6), 065010.
(38) Li, Z.; Zhang, X.; Yuan, T.; Zhang, Y.; Luo, C.; Zhang, J.; Liu, Y.; Fan, W. Addition of platelet-rich plasma to silk fibroin hydrogel bioprinting for cartilage regeneration. *Tissue Engineering Part A* **2020**, *26* (15−16), 886−895.
(39) Abelardo, E. Synthetic material bioinks. In *3D Bioprinting for Reconstructive Surgery*; Elsevier, 2018; pp. 137−144.
(40) Gillispie, G.; Prim, P.; Copus, J.; Fisher, J.; Mikos, A. G.; Yoo, J. J.; Atala, A.; Lee, S. J. Assessment methodologies for extrusion-based bioink printability. *Biofabrication* **2020**, *12* (2), 022003.
(41) Gopinathan, J.; Noh, I. Recent trends in bioinks for 3d printing. *Biomaterials research* **2018**, *22* (1), 11.
(42) Liu, F.; Wang, X. Synthetic polymers for organ 3d printing. *Polymers* **2020**, *12* (8), 1765.
(43) Kundu, J.; Pati, F.; Jeong, Y. H.; Cho, D.-W. Biomaterials for biofabrication of 3d tissue scaffolds. In *Biofabrication*; Elsevier, 2013; pp. 23−46.
(44) Tarafder, S.; Koch, A.; Jun, Y.; Chou, C.; Awadallah, M. R.; Lee, C. H. Micro-precise spatiotemporal delivery system embedded in 3d printing for complex tissue regeneration. *Biofabrication* **2016**, *8* (2), 025003.
(45) Bose, S.; Tarafder, S. Calcium phosphate ceramic systems in growth factor and drug delivery for bone tissue engineering: a review. *Acta biomaterialia* **2012**, *8* (4), 1401−1421.
(46) Akkineni, A. R.; Luo, Y.; Schumacher, M.; Nies, B.; Lode, A.; Gelinsky, M. 3d plotting of growth factor loaded calcium phosphate cement scaffolds. *Acta biomaterialia* **2015**, *27*, 264−274.
(47) Ahlfeld, T.; Akkineni, A. R.; Förster, Y.; Köhler, T.; Knaack, S.; Gelinsky, M.; Lode, A. Design and fabrication of complex scaffolds for bone defect healing: combined 3d plotting of a calcium phosphate cement and a growth factor-loaded hydrogel. *Annals of biomedical engineering* **2017**, *45* (1), 224−236.
(48) Ahlfeld, T.; Schuster, F. P.; Förster, Y.; Quade, M.; Akkineni, A. R.; Rentsch, C.; Rammelt, S.; Gelinsky, M.; Lode, A. 3d plotted biphasic bone scaffolds for growth factor delivery: biological characterization in vitro and in vivo. *Advanced healthcare materials* **2019**, *8* (7), 1801512.
(49) Shim, J.-H.; Kim, S. E.; Park, J. Y.; Kundu, J.; Kim, S. W.; Kang, S. S.; Cho, D.-W. Three-dimensional printing of rhbmp-2-loaded scaffolds with long-term delivery for enhanced bone regeneration in a rabbit diaphyseal defect. *Tissue Engineering Part A* **2014**, *20* (13−14), 1980−1992.
(50) Loozen, L. D.; Wegman, F.; Öner, F. C.; Dhert, W. J.; Alblas, J. Porous bioprinted constructs in bmp-2 non-viral gene therapy for bone tissue engineering. *Journal of Materials Chemistry B* **2013**, *1* (48), 6619−6626.
(51) Gonzalez-Fernandez, T.; Rathan, S.; Hobbs, C.; Pitacco, P.; Freeman, F.; Cunniffe, G.; Dunne, N.; McCarthy, H.; Nicolosi, V.; O'Brien, F.; et al. Pore-forming bioinks to enable spatio-temporally defined gene delivery in bioprinted tissues. *J. Controlled Release* **2019**, *301*, 13−27.
(52) Cunniffe, G. M.; Gonzalez-Fernandez, T.; Daly, A.; Sathy, B. N.; Jeon, O.; Alsberg, E.; Kelly, D. J. Three-dimensional bioprinting of polycaprolactone reinforced gene activated bioinks for bone tissue engineering. *Tissue Engineering Part A* **2017**, *23* (17−18), 891−900.
(53) Bozo, I. Y.; Deev, R. V.; Smirnov, I. V.; Fedotov, A. Y.; Popov, V. K.; Mironov, A. V.; Mironova, O. A.; Gerasimenko, A. Y.; Komlev, V. S. 3d printed gene-activated octacalcium phosphate implants for large bone defects engineering. *International Journal of Bioprinting* **2020**, *6* (3), 275.
(54) Tayalia, P.; Mooney, D. J. Controlled growth factor delivery for tissue engineering. *Advanced materials* **2009**, *21* (32−33), 3269−3285.
(55) Thakur, G.; Rodrigues, F. C.; Singh, K. Crosslinking biopolymers for advanced drug delivery and tissue engineering applications. *Cutting-Edge Enabling Technologies for Regenerative Medicine* **2018**, *1078*, 213−231.
(56) Lee, K.; Silva, E. A.; Mooney, D. J. Growth factor delivery-based tissue engineering: general approaches and a review of recent developments. *Journal of the Royal Society Interface* **2011**, *8* (55), 153−170.
(57) Johnson, B. N.; Lancaster, K. Z.; Zhen, G.; He, J.; Gupta, M. K.; Kong, Y. L.; Engel, E. A.; Krick, K. D.; Ju, A.; Meng, F.; et al. 3d printed anatomical nerve regeneration pathways. *Advanced functional materials* **2015**, *25* (39), 6205−6217.
(58) Park, J. Y.; Shim, J.-H.; Choi, S.-A.; Jang, J.; Kim, M.; Lee, S. H.; Cho, D.-W. 3d printing technology to control bmp-2 and vegf delivery spatially and temporally to promote large-volume bone regeneration. *Journal of Materials Chemistry B* **2015**, *3* (27), 5415−5425.
(59) Ker, E. D.; Nain, A. S.; Weiss, L. E.; Wang, J.; Suhan, J.; Amon, C. H.; Campbell, P. G. Bioprinting of growth factors onto aligned sub-micron fibrous scaffolds for simultaneous control of cell differentiation and alignment. *Biomaterials* **2011**, *32* (32), 8097−8107.
(60) Teixeira, S. P.; Domingues, R. M.; Shevchuk, M.; Gomes, M. E.; Peppas, N. A.; Reis, R. L. Biomaterials for sequestration of growth factors and modulation of cell behavior. *Advanced Functional Materials* **2020**, *30* (44), 1909011.
(61) Park, J.; Lee, S. J.; Lee, H.; Park, S. A.; Lee, J. Y. Three dimensional cell printing with sulfated alginate for improved bone morphogenetic protein-2 delivery and osteogenesis in bone tissue engineering. *Carbohydrate polymers* **2018**, *196*, 217−224.
(62) Hajimiri, M.; Shahverdi, S.; Kamalinia, G.; Dinarvand, R. Growth factor conjugation: strategies and applications. *Journal of biomedical materials research Part A* **2015**, *103* (2), 819−838.
(63) Byambaa, B.; Annabi, N.; Yue, K.; Trujillo-de Santiago, G.; Alvarez, M. M.; Jia, W.; Kazemzadeh-Narbat, M.; Shin, S. R.; Tamayol, A.; Khademhosseini, A. Bioprinted osteogenic and vasculogenic patterns for engineering 3d bone tissue. *Advanced healthcare materials* **2017**, *6* (16), 1700015.
(64) Carrow, J. K.; Kerativitayanan, P.; Jaiswal, M. K.; Lokhande, G.; Gaharwar, A. K. Polymers for bioprinting. In *Essentials of 3D biofabrication and translation*; Elsevier, 2015; pp. 229−248.
(65) Chimene, D.; Kaunas, R.; Gaharwar, A. K. Hydrogel bioink reinforcement for additive manufacturing: a focused review of emerging strategies. *Advanced materials* **2020**, *32* (1), 1902026.
(66) Ahlfeld, T.; Cidonio, G.; Kilian, D.; Duin, S.; Akkineni, A.; Dawson, J.; Yang, S.; Lode, A.; Oreffo, R.; Gelinsky, M. Development of a clay based bioink for 3d cell printing for skeletal application. *Biofabrication* **2017**, *9* (3), 034103.
(67) Chu, C.; Deng, J.; Liu, L.; Cao, Y.; Wei, X.; Li, J.; Man, Y. Nanoparticles combined with growth factors: recent progress and applications. *Rsc Advances* **2016**, *6* (93), 90856−90872.
(68) Elkhoury, K.; Russell, C. S.; Sanchez-Gonzalez, L.; Mostafavi, A.; Williams, T. J.; Kahn, C.; Peppas, N. A.; Arab-Tehrany, E.; Tamayol, A. Soft-nanoparticle functionalization of natural hydrogels for tissue

https://doi.org/10.1021/acsbiomaterials.3c00873
ACS Biomater. Sci. Eng. 2023, 9, 6531−6547

engineering applications. *Advanced healthcare materials* **2019**, *8* (18), 1900506.
(69) Peak, C. W.; Singh, K. A.; Adlouni, M.; Chen, J.; Gaharwar, A. K. Printing therapeutic proteins in 3d using nanoengineered bioink to control and direct cell migration. *Advanced healthcare materials* **2019**, *8* (11), 1801553.
(70) Sun, B.; Lian, M.; Han, Y.; Mo, X.; Jiang, W.; Qiao, Z.; Dai, K. A 3d-bioprinted dual growth factor-releasing intervertebral disc scaffold induces nucleus pulposus and annulus fibrosus reconstruction. *Bioactive materials* **2021**, *6* (1), 179−190.
(71) Freeman, F. E.; Pitacco, P.; van Dommelen, L. H.; Nulty, J.; Browe, D. C.; Shin, J.-Y.; Alsberg, E.; Kelly, D. J. 3d bioprinting spatiotemporally defined patterns of growth factors to tightly control tissue regeneration. *Science advances* **2020**, *6* (33), No. eabb5093.
(72) Lee, S.-J.; Zhu, W.; Heyburn, L.; Nowicki, M.; Harris, B.; Zhang, L. G. Development of novel 3-d printed scaffolds with core-shell nanoparticles for nerve regeneration. *IEEE Transactions on Biomedical Engineering* **2017**, *64* (2), 408−418.
(73) Hossain, K. M. Z.; Patel, U.; Ahmed, I. Development of microspheres for biomedical applications: a review. *Progress in biomaterials* **2015**, *4* (1), 1−19.
(74) Varde, N. K.; Pack, D. W. Microspheres for controlled release drug delivery. *Expert opinion on biological therapy* **2004**, *4* (1), 35−51.
(75) Kim, K. K.; Pack, D. W. Microspheres for drug delivery. In *BioMEMS and Biomedical Nanotechnology*; Springer, 2006; pp. 19−50.
(76) Poldervaart, M. T.; Gremmels, H.; van Deventer, K.; Fledderus, J. O.; Öner, F. C.; Verhaar, M. C.; Dhert, W. J.; Alblas, J. Prolonged presence of vegf promotes vascularization in 3d bioprinted scaffolds with defined architecture. *Journal of controlled release* **2014**, *184*, 58−66.
(77) Makadia, H. K.; Siegel, S. J. Poly lactic-co-glycolic acid (plga) as biodegradable controlled drug delivery carrier. *Polymers* **2011**, *3* (3), 1377−1397.
(78) Dawes, G.; Fratila-Apachitei, L.; Mulia, K.; Apachitei, I.; Witkamp, G.-J.; Duszczyk, J. Size effect of plga spheres on drug loading efficiency and release profiles. *Journal of Materials Science: Materials in Medicine* **2009**, *20* (5), 1089−1094.
(79) Klose, D.; Siepmann, F.; Elkharraz, K.; Krenzlin, S.; Siepmann, J. How porosity and size affect the drug release mechanisms from plga-based microparticles. *International journal of pharmaceutics* **2006**, *314* (2), 198−206.
(80) Swider, E.; Koshkina, O.; Tel, J.; Cruz, L. J.; de Vries, I. J. M.; Srinivas, M. Customizing poly (lactic-co-glycolic acid) particles for biomedical applications. *Acta biomaterialia* **2018**, *73*, 38−51.
(81) Lee, C. H.; Rodeo, S. A.; Fortier, L. A.; Lu, C.; Erisken, C.; Mao, J. J. Protein-releasing polymeric scaffolds induce fibrochondrocytic differentiation of endogenous cells for knee meniscus regeneration in sheep. *Science translational medicine* **2014**, *6* (266), 266ra171.
(82) Sun, Y.; You, Y.; Jiang, W.; Wang, B.; Wu, Q.; Dai, K. 3d bioprinting dual-factor releasing and gradient-structured constructs ready to implant for anisotropic cartilage regeneration. *Science Advances* **2020**, *6* (37), No. eaay1422.
(83) Hosseinzadeh, R.; Mirani, B.; Pagan, E.; Mirzaaghaei, S.; Nasimian, A.; Kawalec, P.; da Silva Rosa, S. C.; Hamdi, D.; Fernandez, N. P.; Toyota, B. D.; et al. A drug-eluting 3d-printed mesh (gliomesh) for management of glioblastoma. *Advanced Therapeutics* **2019**, *2* (11), 1900113.
(84) Rehmann, M. S.; Skeens, K. M.; Kharkar, P. M.; Ford, E. M.; Maverakis, E.; Lee, K. H.; Kloxin, A. M. Tuning and predicting mesh size and protein release from step growth hydrogels. *Biomacromolecules* **2017**, *18* (10), 3131−3142.
(85) Kilian, D.; Cometta, S.; Bernhardt, A.; Taymour, R.; Golde, J.; Ahlfeld, T.; Emmermacher, J.; Gelinsky, M.; Lode, A. Core−shell bioprinting as a strategy to apply differentiation factors in a spatially defined manner inside osteochondral tissue substitutes. *Biofabrication* **2022**, *14* (1), 014108.
(86) Petcu, E. B.; Midha, R.; McColl, E.; Popa-Wagner, A.; Chirila, T. V.; Dalton, P. D. 3d printing strategies for peripheral nerve regeneration. *Biofabrication* **2018**, *10* (3), 032001.
(87) Amini, A. R.; Laurencin, C. T.; Nukavarapu, S. P. Bone tissue engineering: recent advances and challenges. *Critical Reviews in Biomedical Engineering* **2012**, *40* (5), 363.
(88) Genova, T.; Petrillo, S.; Zicola, E.; Roato, I.; Ferracini, R.; Tolosano, E.; Altruda, F.; Carossa, S.; Mussano, F.; Munaron, L. The crosstalk between osteodifferentiating stem cells and endothelial cells promotes angiogenesis and bone formation. *Frontiers in physiology* **2019**, *10*, 1291.
(89) Gonçalves, R. C.; Banfi, A.; Oliveira, M. B.; Mano, J. F. Strategies for re-vascularization and promotion of angiogenesis in trauma and disease. *Biomaterials* **2021**, *269*, 120628.
(90) Oliveira, É. R.; Nie, L.; Podstawczyk, D.; Allahbakhsh, A.; Ratnayake, J.; Brasil, D. L.; Shavandi, A. Advances in growth factor delivery for bone tissue engineering. *International Journal of Molecular Sciences* **2021**, *22* (2), 903.
(91) Santo, V. E.; Gomes, M. E.; Mano, J. F.; Reis, R. L. Controlled release strategies for bone, cartilage, and osteochondral engineering—part i: recapitulation of native tissue healing and variables for the design of delivery systems. *Tissue Engineering Part B: Reviews* **2013**, *19* (4), 308−326.
(92) De Witte, T.-M.; Fratila-Apachitei, L. E.; Zadpoor, A. A.; Peppas, N. A. Bone tissue engineering via growth factor delivery: from scaffolds to complex matrices. *Regenerative biomaterials* **2018**, *5* (4), 197−211.
(93) Chen, S.; Shi, Y.; Zhang, X.; Ma, J. Evaluation of bmp-2 and vegf loaded 3d printed hydroxyapatite composite scaffolds with enhanced osteogenic capacity in vitro and in vivo. *Materials Science and Engineering: C* **2020**, *112*, 110893.
(94) Kempen, D. H.; Lu, L.; Heijink, A.; Hefferan, T. E.; Creemers, L. B.; Maran, A.; Yaszemski, M. J.; Dhert, W. J. Effect of local sequential vegf and bmp-2 delivery on ectopic and orthotopic bone regeneration. *Biomaterials* **2009**, *30* (14), 2816−2825.
(95) Wang, Q.; Zhang, Y.; Li, B.; Chen, L. Controlled dual delivery of low doses of bmp-2 and vegf in a silk fibroin−nanohydroxyapatite scaffold for vascularized bone regeneration. *Journal of Materials Chemistry B* **2017**, *5* (33), 6963−6972.
(96) Young, S.; Patel, Z. S.; Kretlow, J. D.; Murphy, M. B.; Mountziaris, P. M.; Baggett, L. S.; Ueda, H.; Tabata, Y.; Jansen, J. A.; Wong, M.; et al. Dose effect of dual delivery of vascular endothelial growth factor and bone morphogenetic protein-2 on bone regeneration in a rat critical-size defect model. *Tissue Engineering Part A* **2009**, *15* (9), 2347−2362.
(97) Kjar, A.; McFarland, B.; Mecham, K.; Harward, N.; Huang, Y. Engineering of tissue constructs using coaxial bioprinting. *Bioactive materials* **2021**, *6* (2), 460−471.
(98) Zhang, Y.; Yu, Y.; Akkouch, A.; Dababneh, A.; Dolati, F.; Ozbolat, I. T. In vitro study of directly bioprinted perfusable vasculature conduits. *Biomaterials science* **2015**, *3* (1), 134−143.
(99) Akkineni, A. R.; Ahlfeld, T.; Lode, A.; Gelinsky, M. A versatile method for combining different biopolymers in a core/shell fashion by 3d plotting to achieve mechanically robust constructs. *Biofabrication* **2016**, *8* (4), 045001.
(100) O'Donnell, B. T.; Ives, C. J.; Mohiuddin, O. A.; Bunnell, B. A. Beyond the present constraints that prevent a wide spread of tissue engineering and regenerative medicine approaches. *Frontiers in bioengineering and biotechnology* **2019**, *7*, 95.

https://doi.org/10.1021/acsbiomaterials.3c00873
ACS Biomater. Sci. Eng. 2023, 9, 6531−6547